No. 15. INFRARED SPECTRA OF STARS AND PLANETS, I: PHOTOMETRY OF THE INFRARED SPECTRUM OF VENUS, 1–2.5 MICRONS

by GERARD P. KUIPER

October 26, 1962

1. Introduction

THE spectrum of Venus beyond the photographic range has been investigated with resolutions of about 250 up to 1.8μ (Kuiper, 1948), 80 up to 2.5μ (Kuiper, 1947), and about 30 for the range 8-14μ (Sinton, 1962). Recently Gebbie, Delbouille, and Roland (1962) recorded the region 1.2-2.5μ with an interferometer and obtained a spectral resolution similar to that used by Kuiper. Some inconsistencies are apparent between these provisional interferometer results and the earlier direct tracings.

From time to time during the past decade, the writer had attempted to improve on his 1948 results with the prism spectrometer, but no distinct progress was made until a grating spectrometer was built which allowed increased resolution without undue loss of light. This new instrument is described in No. 16 of these *Communications*. With it, the Venus spectrum in the region 1.0-2.5μ has been recorded in two series, one obtained with the 36-inch telescope of the Kitt Peak National Observatory in June 1962 (resolutions about 700 and 250), and one with the 82-inch telescope of the McDonald Observatory in August 1962 (resolutions about 1500 and 800). The Kitt Peak series was supplemented with matching solar comparison runs, so that fairly precise photometric determinations of the Venus absorptions could be made. The McDonald series was calibrated with lunar spectra for the regions 1.2-1.4μ and 1.9-2.5μ, and stellar spectra for the remaining regions; these spectra by their nature do not have the highest precision for defining the continuous spectrum. Solar spectra obtained in Tucson are to be added later as supplementary comparison standards. The wavelengths of the telluric absorptions were taken from the McMath-Hulbert Observatory Atlas (1950).

The spectral records reproduced are photometric since the intensity scales are known to be strictly linear. The absorption depths and equivalent widths can therefore be taken directly from the spectra.

Nearly forty absorption bands were found in the Venus spectrum between 1.0-2.5μ. All of these without exception could be attributed to CO_2. A survey of possible CO_2 bands showed that all bands up to a certain intensity that should be present in the Venus spectrum are indeed present. Several bands of the heavy carbon isotope $^{13}CO_2$ have been identified as well as a number of "hot" bands of $^{12}CO_2$. Some weaker features shown in both the laboratory spectra and Venus and apparently due to CO_2 have been left unidentified. One fairly strong band, at $\lambda = 2.15\mu$, appeared to be outside the scheme of permitted transitions of $^{12}CO_2$, and is attributed, not to the $2\nu_3$ band of $^{12}C^{16}O^{16}O$, which is forbidden, but to its heavy-oxygen, ^{18}O, isotopic companion, $^{12}C^{18}O^{16}O$, which is permitted. Because the principal band is forbidden the isotopic band can be observed with unusual freedom from interference.

2. The Kitt Peak Spectra

The original records obtained, with wavelength marks added, are reproduced photographically in Figures 1-6 (the only record omitted is the solar comparison for 1.0-1.35μ, used in Figure 1, full reproduction of which seemed unnecessary).

The resolution of the spectra is not the same for the two intervals 1.0-1.8μ and 1.9-2.5μ. In each

case the spectrometer was used in slitless form to minimize intensity fluctuations due to seeing or guiding. The planetary disk was about 0.80 illuminated, with the narrow dimension 10″ in width. The spectrometer was turned so that this narrow dimension served as the entrance slit. With the Kitt Peak 36-inch telescope, f/15 Cassegrain, this meant that the equivalent slit was 2/3 mm, or actually slightly less, because of the curvature of the planet and the uneven illumination of the disk. The cell width used for 1.0-1.8μ was 0.25 mm, so that the resolution in the spectrum was about $\sqrt{(2/3)^2 + (0.25)^2} = 0.7$ mm, that is, $\lambda/\Delta\lambda \cong 700$ at 1.6μ, giving $\Delta\lambda \cong 25$A. From 1.9-2.5μ a 1.0 mm cell was used to improve the signal/noise ratio. This means that the spectral resolution there was about $\sqrt{(2/3)^2 + 1} = 1.2$ mm; and because the dispersion with the 2μ grating is only 0.4 times that of the 1.6μ grating, the overall spectral resolution was $(1.2/0.7) / 0.4 = 4.3$ times poorer, i.e., about 100A or $\lambda / \Delta\lambda = 200$ at 2.2μ. These computed resolutions are approximately confirmed by the spectra themselves except that Figures 4 and 5 may suggest a resolution slightly better than 0.01μ.

The chief interest of the spectra is, of course, to obtain a listing and identification of the planetary absorptions. The Kitt Peak records are clear for all but a few of the CO_2 bands marked. These marginal cases are recognized more easily with the increased resolution obtained in the McDonald spectra. There is no evidence for an absorption between 2.3 and 2.4μ which could be attributed to CO. Between 2.2-2.3μ there is in Figure 4 a feature which, if real, indicates a local color difference between Venus and the Sun, attributable to the Venus cloud cover. The question arises whether this feature could be due to small ice crystals in the Venus atmosphere. To check this, reflection spectra were obtained of sunlight shining on small H_2O crystals formed on a dark metal plate in contact with a block of frozen CO_2 and matched with the solar spectrum reflected from a MgO block. The records are reproduced in Figure 7*a*, and the ratios between the ordinates measured at identifiable wavelengths are plotted in Figure 7*b*. It is seen that the ice causes a wide absorption band from 1.9-2.1μ, and another one beyond 2.4μ, increasing in strength with increasing depth of the layer; but that the absorption is least between 2.2-2.3μ, where the suspected Venus absorption occurs. The ice band is displaced from the corresponding vapor band by about + 0.1μ, in accordance with previous laboratory work. It is seen from Figure 4 that the Venus spectrum from 1.88-1.93μ and the peak at 1.98μ are incompatible with the ice band at 2.0μ shown in Figure 7*b*.

3. *The McDonald Spectra*

The Kitt Peak spectra had been obtained toward the close of the spring season in the U.S. Southwest, when the daytime mountain temperatures were already fairly high (20°-25°C), but the relative humidities still low (10-15%) and the skies beautifully photometric.

The McDonald run in August took place during the rainy season, but in 1962 substantial breaks occurred of comparatively low humidity (30-40%) and excellent observing conditions, even during some afternoons (when normally thunderstorm cumuli are present over the mountains). During these daytime runs the image quality in the 82-inch telescope was often surprisingly good (3 or better on a scale of 5), making it possible to use a fairly narrow slit (0.3 mm) and yet have a nearly constant light source. The best results were obtained by keeping the slit East-West, and by placing the planetary image, now close to dichotomy, as nearly as possible symmetrically on the slit. Accurate guiding in RA was maintained, and the slow drift in declination was corrected periodically, by hand, without harmful effects on the transmitted intensity, owing to the large size of the image in declination (> 3 mm). A 0.1 mm cell was used throughout so that the equivalent spectral resolution was 0.32 mm, making $\lambda/\Delta\lambda \cong 1500$ at 1.6μ, or $\Delta\lambda \simeq 10$A. Inspection of the spectral records confirms this value. For 1.9-2.5μ the 2μ grating was used again, but with the same narrow cell and slit as used at 1.6μ; the resolution was thus about 25A and $\lambda/\Delta\lambda$ about 800-1000. However, the smaller ratio signal/noise in this region caused some loss of effective resolution which could be recaptured only by the use of a longer time constant and a slower scanning rate.

Because solar comparison runs with the spectrometer on or off the 82-inch telescope could not be made during a full-time night program, the calibration of the McDonald spectra on Venus had to be left somewhat incomplete. Night-time lunar spectra were taken for the 1.18-1.35μ and 1.9-2.5μ regions, which served as a first approximation. They were obtained by throwing the lunar image on the spectrometer slit far out of focus so that the unavoidable drift of the image would cause only comparatively small and smooth spurious intensity changes

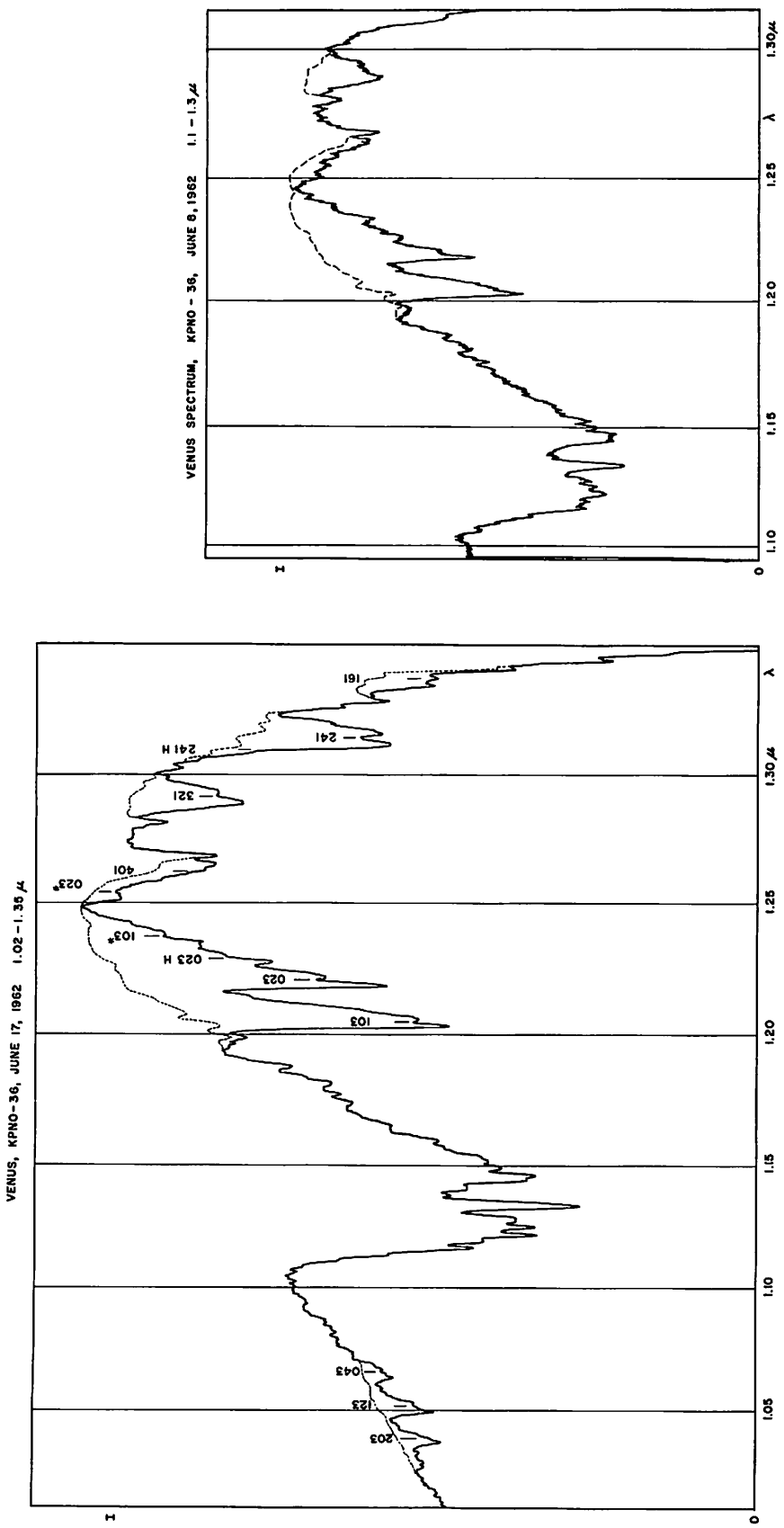

Fig. 1. (*a*) Venus spectrum, Kitt Peak National Observatory, 1.02-1.35μ. Upper curve outlines solar comparison spectrum where it differs from the Venus spectrum. Classification of CO_2 bands follows Table 1, with short lines marking band origins (not heads); *H* designates "hot" bands, asterisk isotopic $^{13}CO_2$ bands. Grating 1.6μ, filter Corning 2540 ($\lambda > 1.0\mu$), cell width 0.25 mm, slitless spectrum, time constant (τ) 12 seconds. Declination of Venus +21°49′, hour angle 1^h49^m-2^h44^mW (in all spectral records the time runs from *right* to *left*). (*b*) Supplementary Venus spectrum, 1.1-1.3μ, same parameters except $\tau = 3$ seconds; Decl. +23°44′, H.A. 0^h55^m-1^h09^mW.

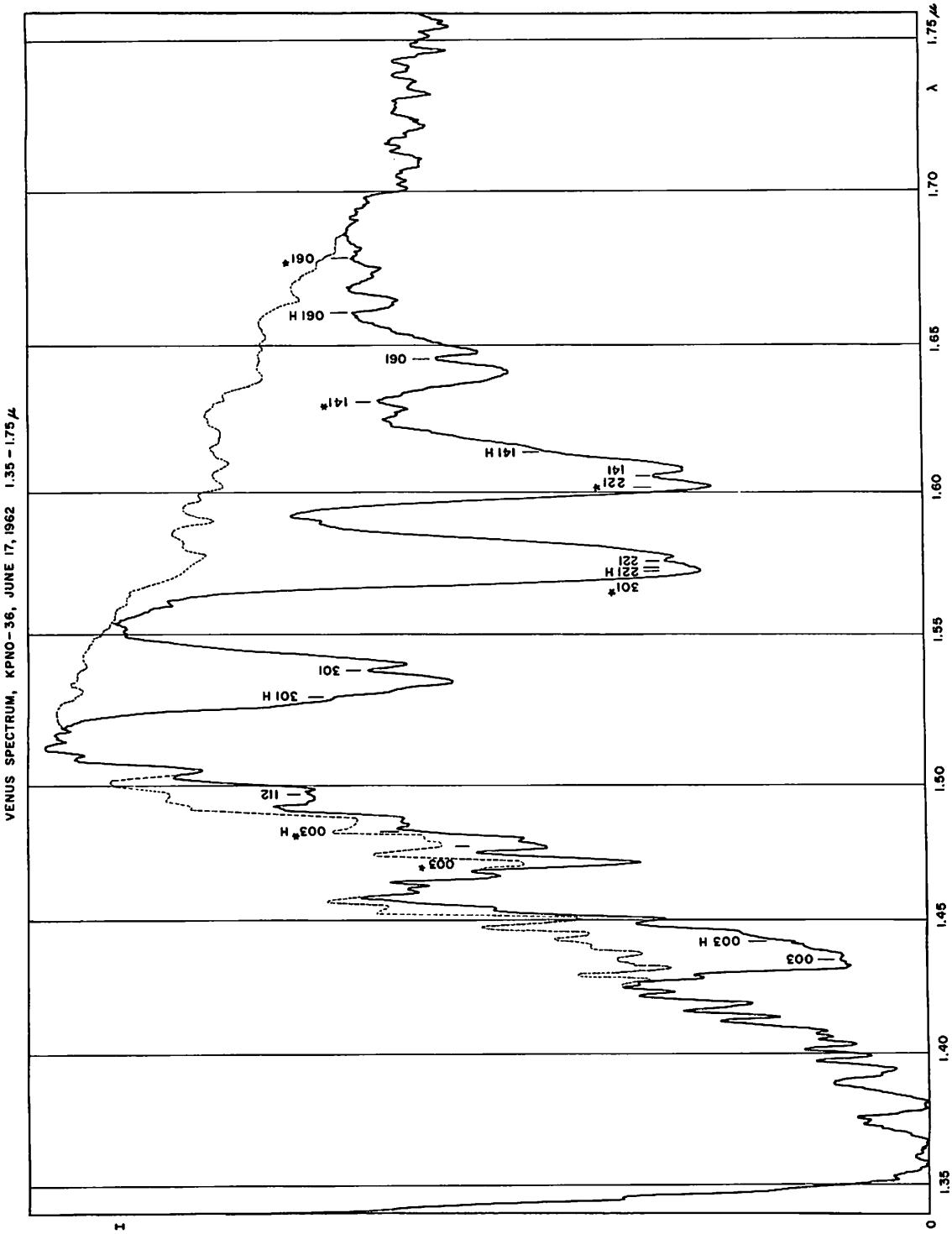

Fig. 2. Venus spectrum, 1.35-1.75μ. Upper curve is solar spectrum shown in Figure 3. CO_2 bands as in Table 1. Same parameters as Figure 1*a* except H.A. 0^h27^m-1^h40^mW.

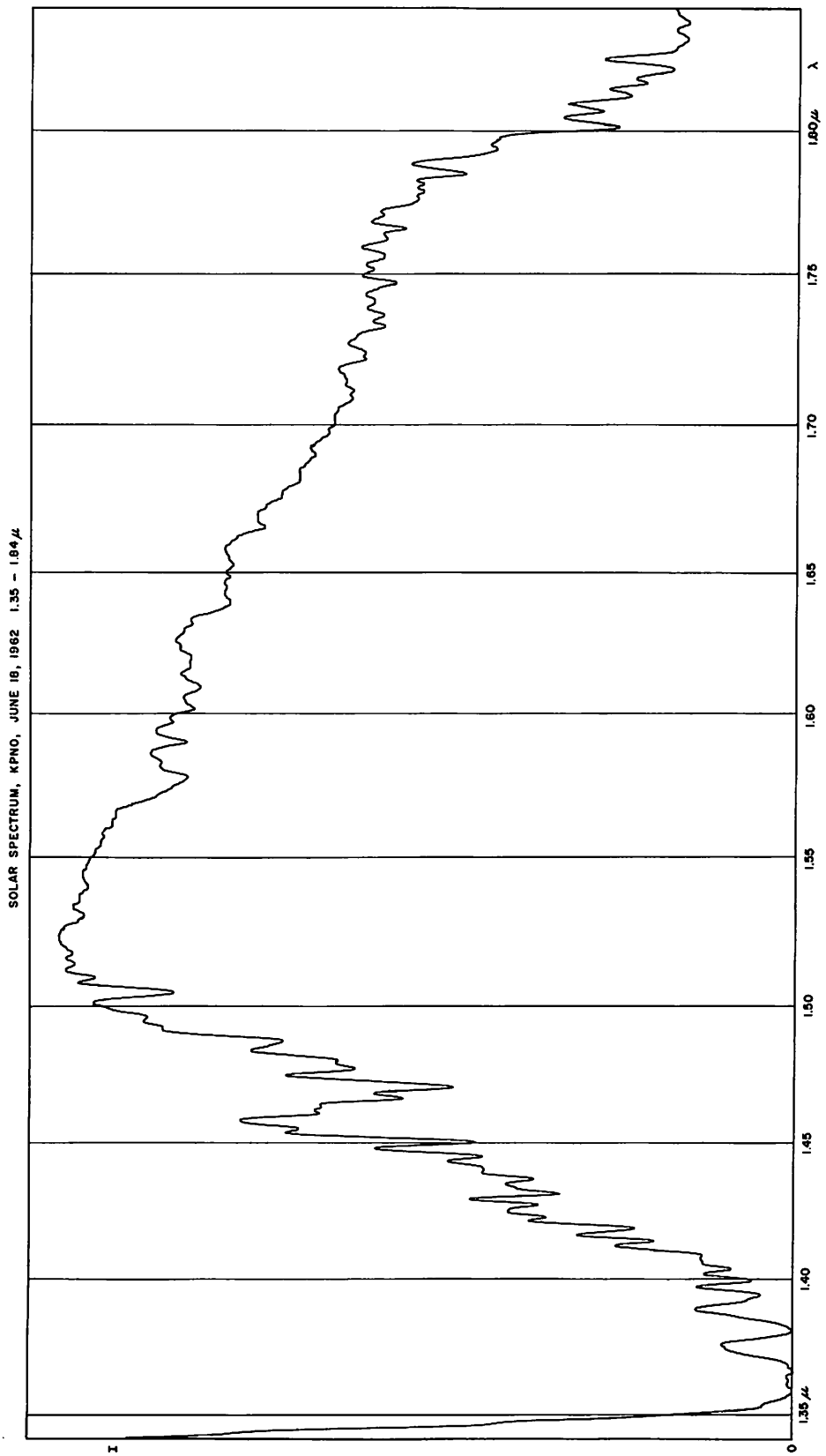

Fig. 3. Solar comparison, 1.35-1.84μ, used in Figure 2. Parameters as in Figure 2 except slitwidth 0.6 mm (the width of the Venus image). Decl. of Sun $+23°24'$, H.A. 0^h37^m-2^h06^mW.

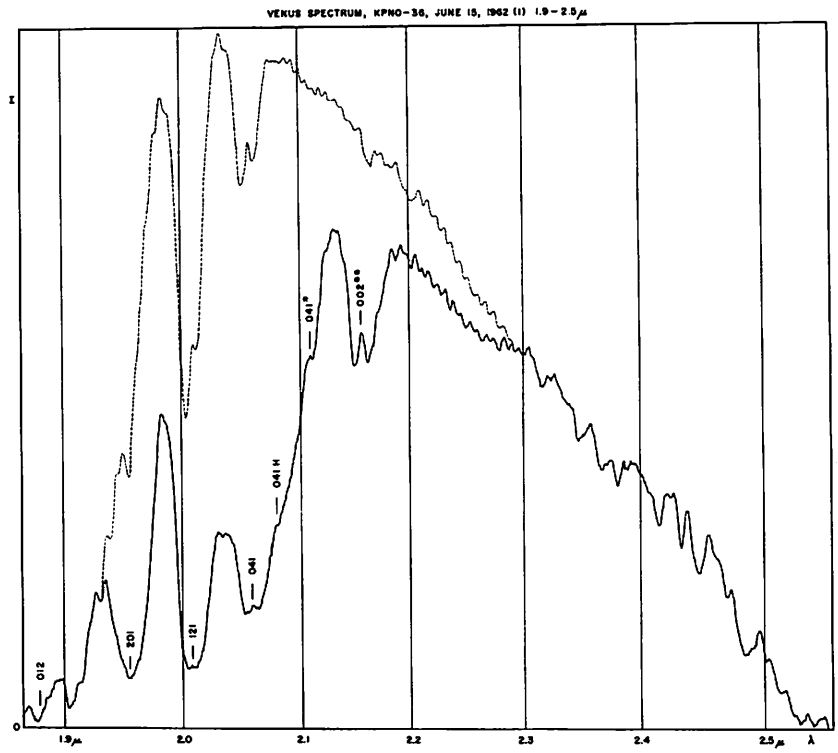

Fig. 4. Venus spectrum, 1.87-2.55μ. Upper curve is solar comparison shown in Figure 5. Grating 2μ, filter $\lambda > 1.9\mu$, cell 1.0 mm, slitless, $\tau = 6$ seconds. Decl. $+22°20'$, H.A. 0^h46^m-1^h11^mW. Double asterisk designates ^{18}O isotopic band. Minor ripples 2.1-2.3μ due to interference between filters.

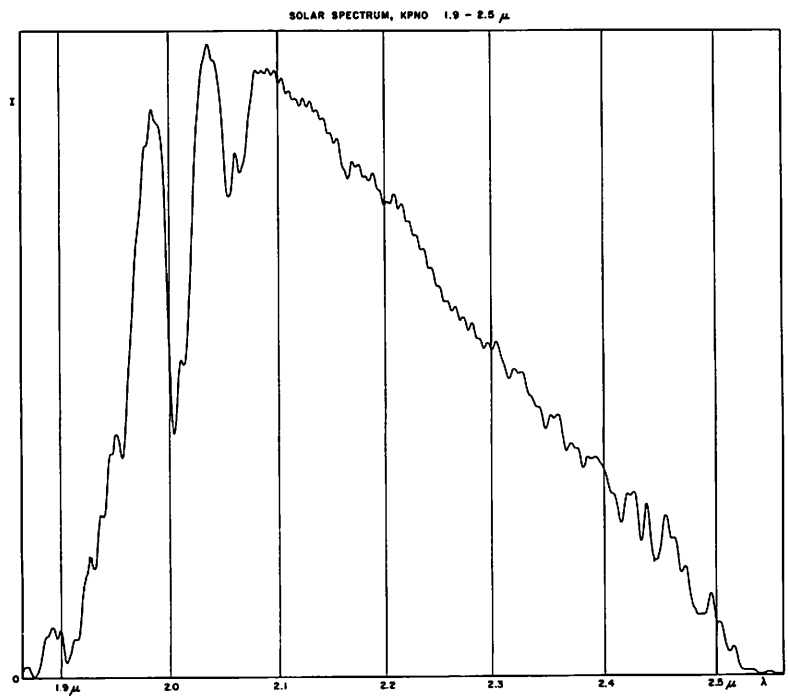

Fig. 5. Solar comparison for Figure 4. Parameters as there except slitwidth 0.6 mm (equal to Venus image). Decl. $+23°21'$, H.A. 0^h49^m-1^h12^mW.

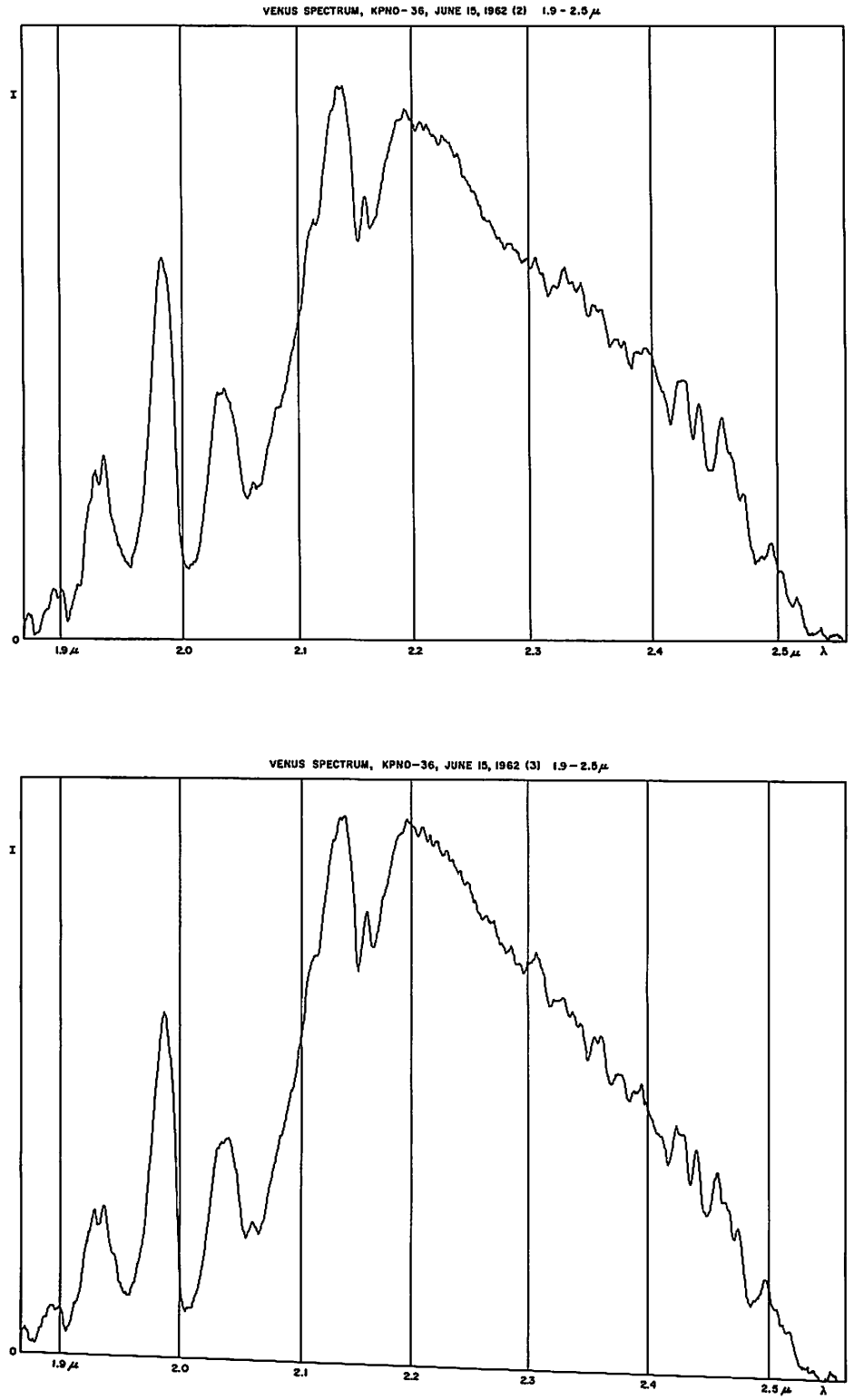

Fig. 6. Additional Venus spectra, 1.9-2.5μ. Parameters as in Figure 4 except (*a*) H.A. 1^h26^m-1^h50^mW; (*b*) H.A. 1^h59^m-2^h12^mW.

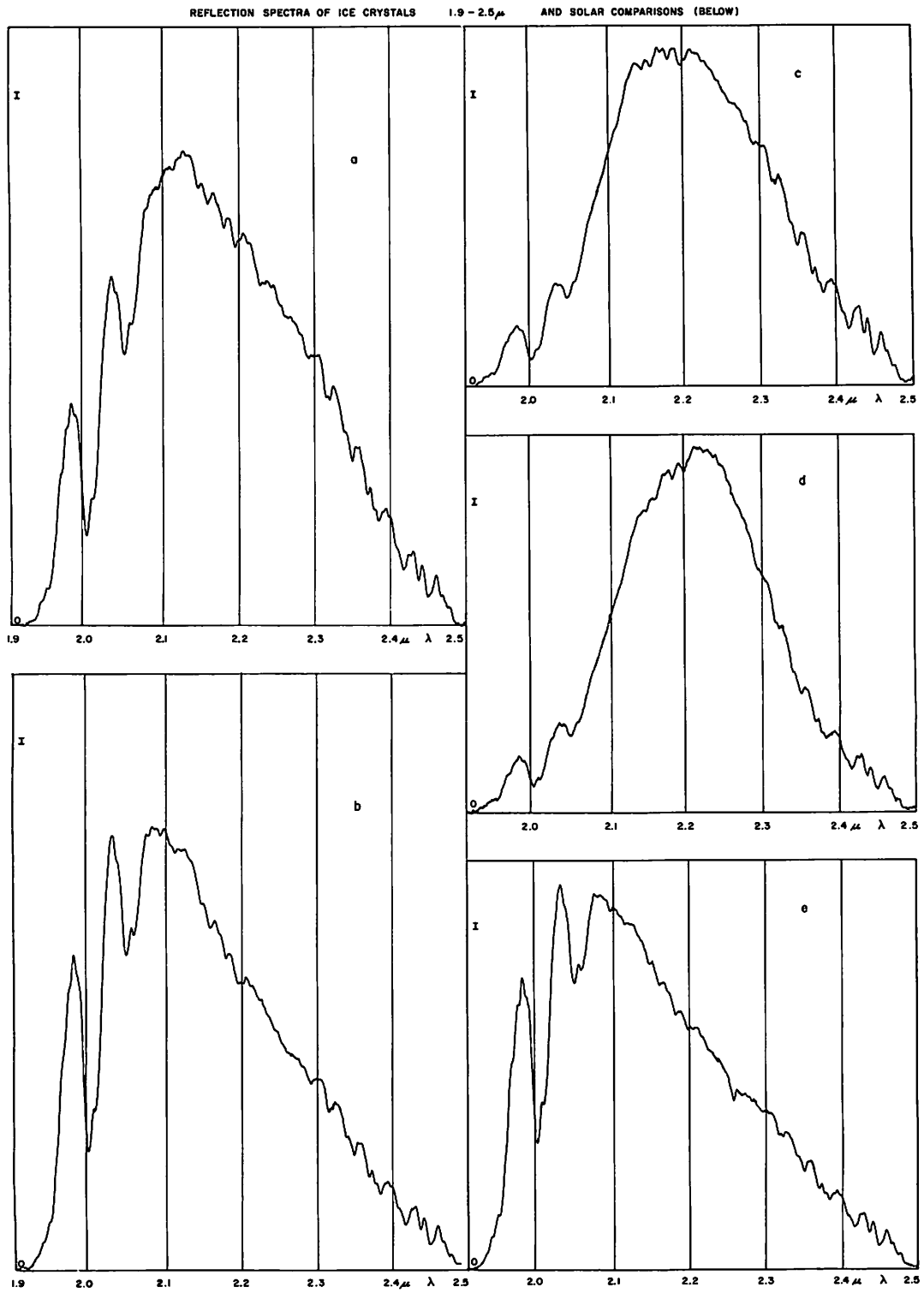

Fig. 7a. Spectra 1.9-2.5μ of sunlight reflected by a layer of small H_2O crystals formed on a dark metal plate cooled by contact with a block of frozen CO_2. Tucson, September 11, 1962, early afternoon; (*a*) crystal layer about 1 mm thick; (*b*) solar comparison as reflected by MgO block; (*c*) frost layer about 3 mm thick; (*d*) frost layer about 4 mm thick; (e) second solar comparison.

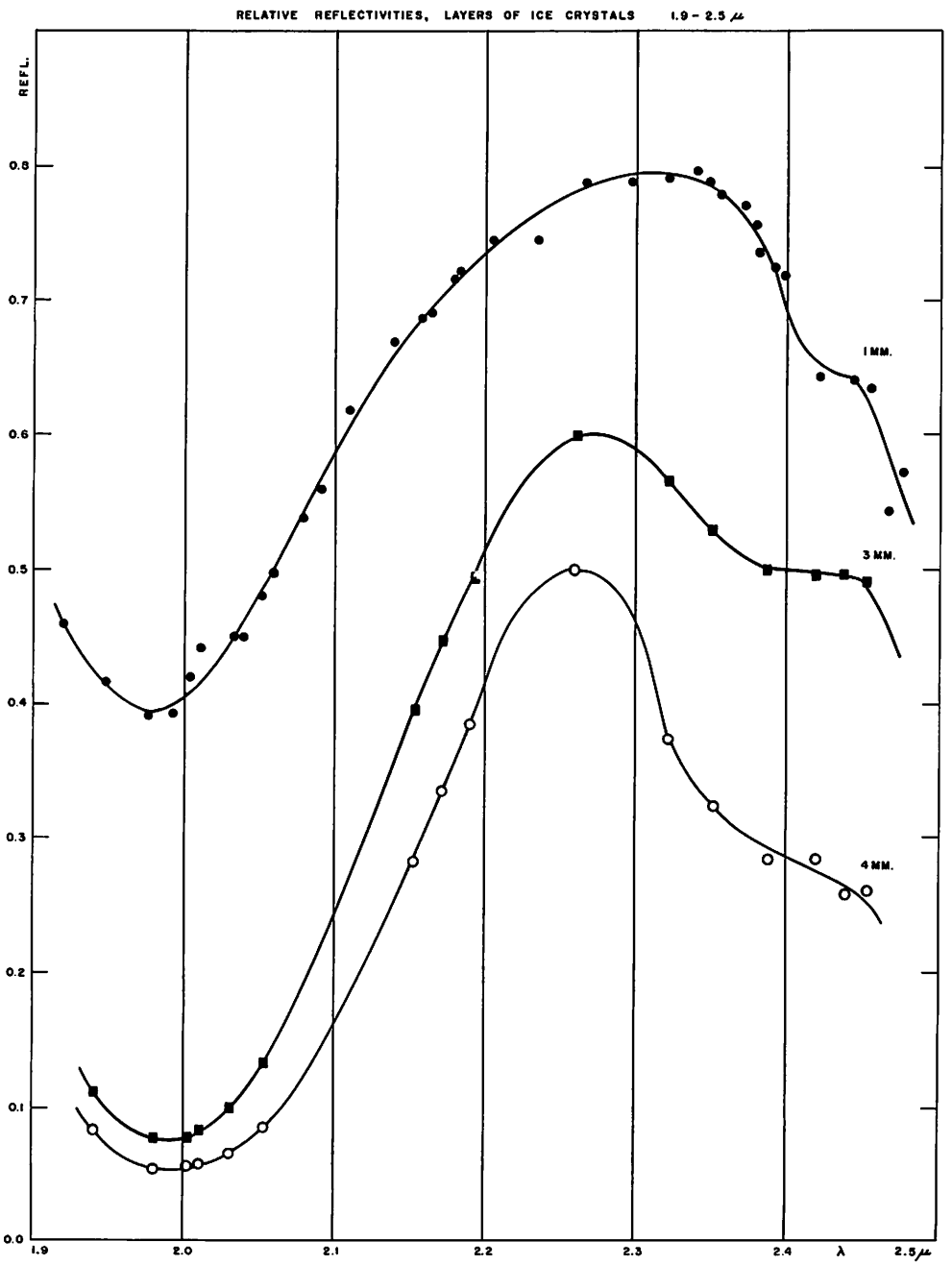

Fig. 7b. Reflectivities of layers of ice crystals 1 mm, 3 mm, and 4 mm thick, derived from Figure 7*a*. The *shapes* of the curves are fixed by the ratios measured from Figure 7*a*; the scales of the ordinates cannot be found from the measures and have been chosen somewhat arbitrarily.

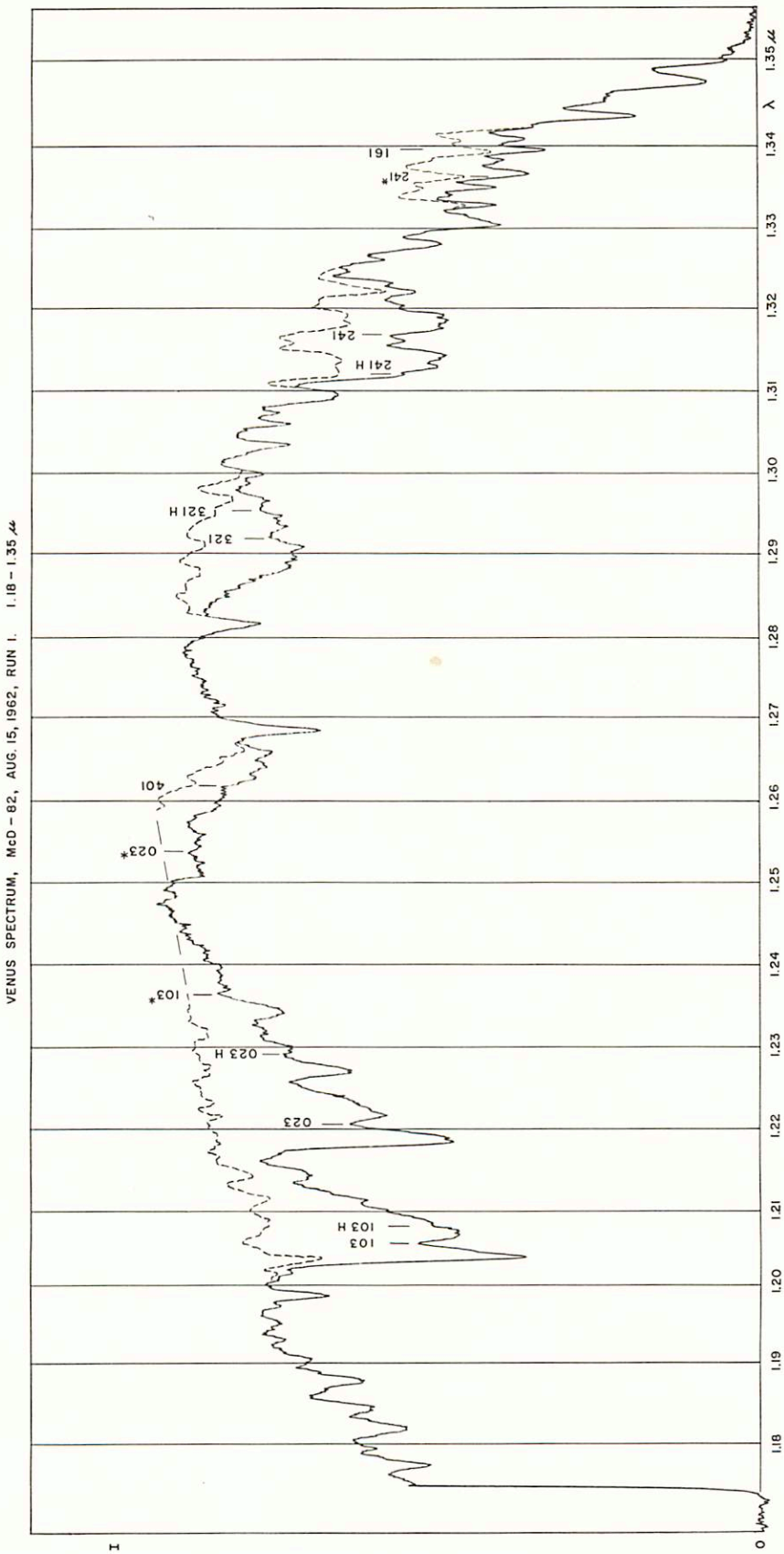

Fig. 8. Venus spectrum, McDonald Observatory, 1.18-1.35μ. Dashes outline lunar comparison spectrum (which was somewhat disturbed from 1.24-1.26μ by relocation of the lunar image). CO_2 bands as in Figure 1. Grating 1.6μ, filter Corning 2540, cell 0.25 mm, slit 0.3 mm, $\tau = 3$ seconds. Decl. $-3°\,39'$, H.A. 0^h34^mE - $0^h0]^m$W. Dome temperature (T) 23°C, humidity (H) 36%.

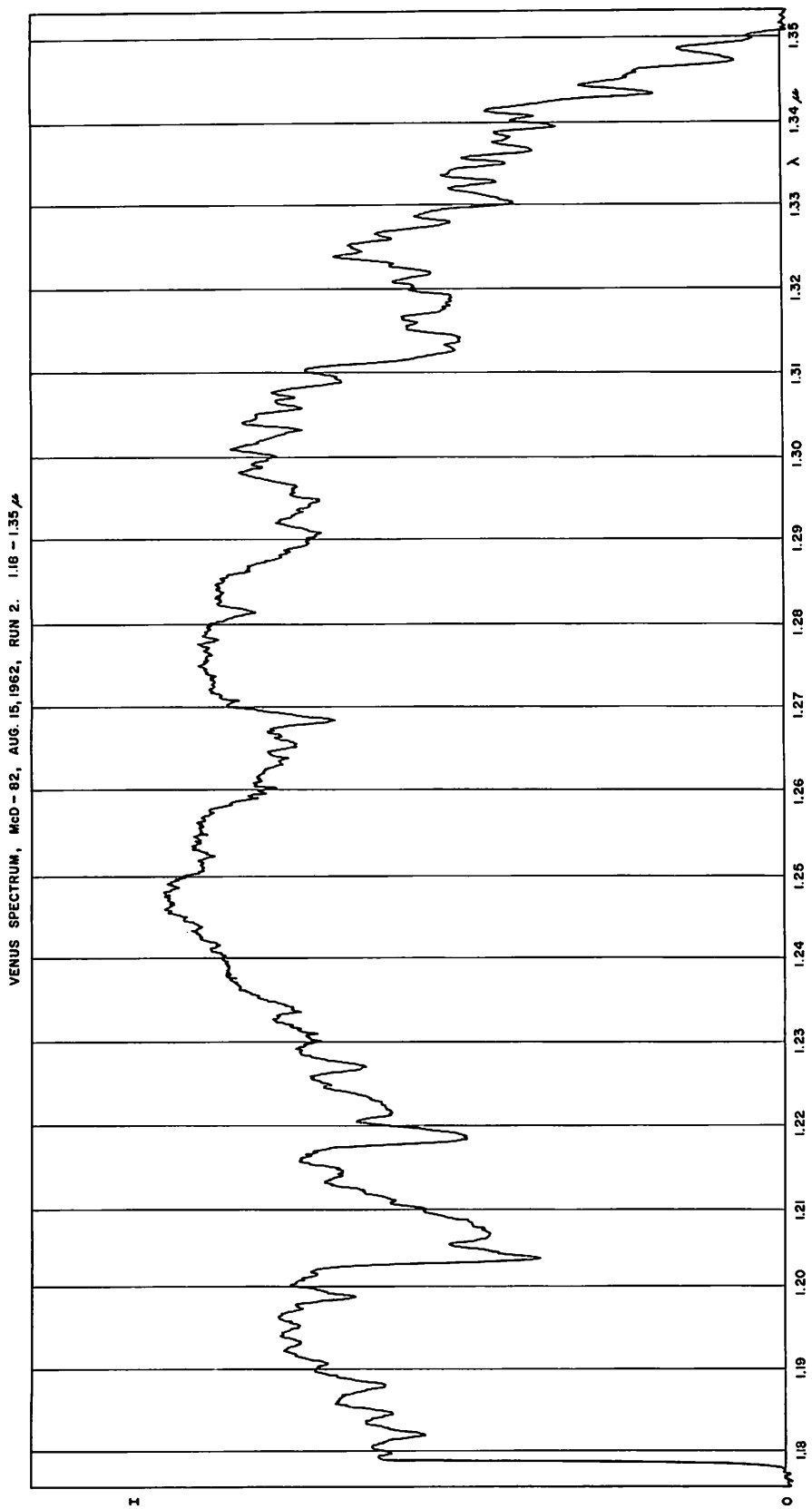

Fig. 9. As Figure 8, H.A. $0^h02^mW - 0^h35^mW$.

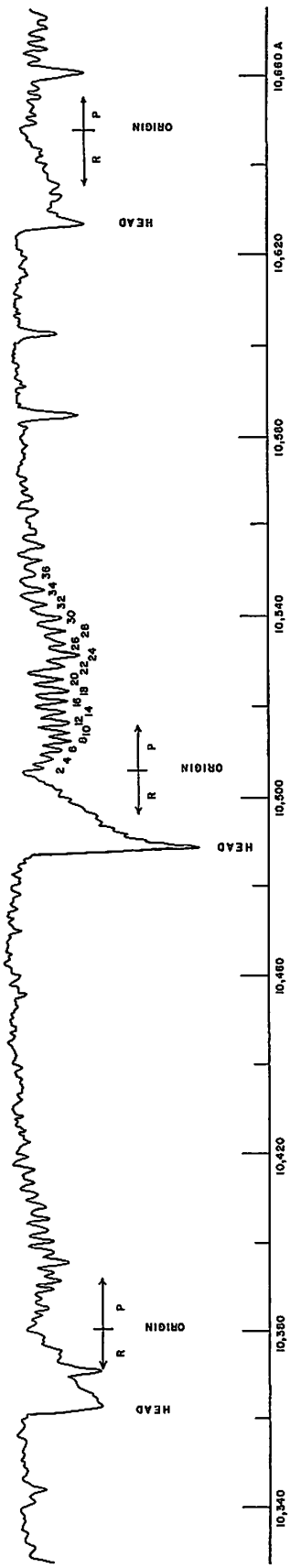

Fig. 10. Microphotometer tracing of the (043, 123, 203) bands of CO_2 in Venus (Chamberlain and Kuiper, 1956).

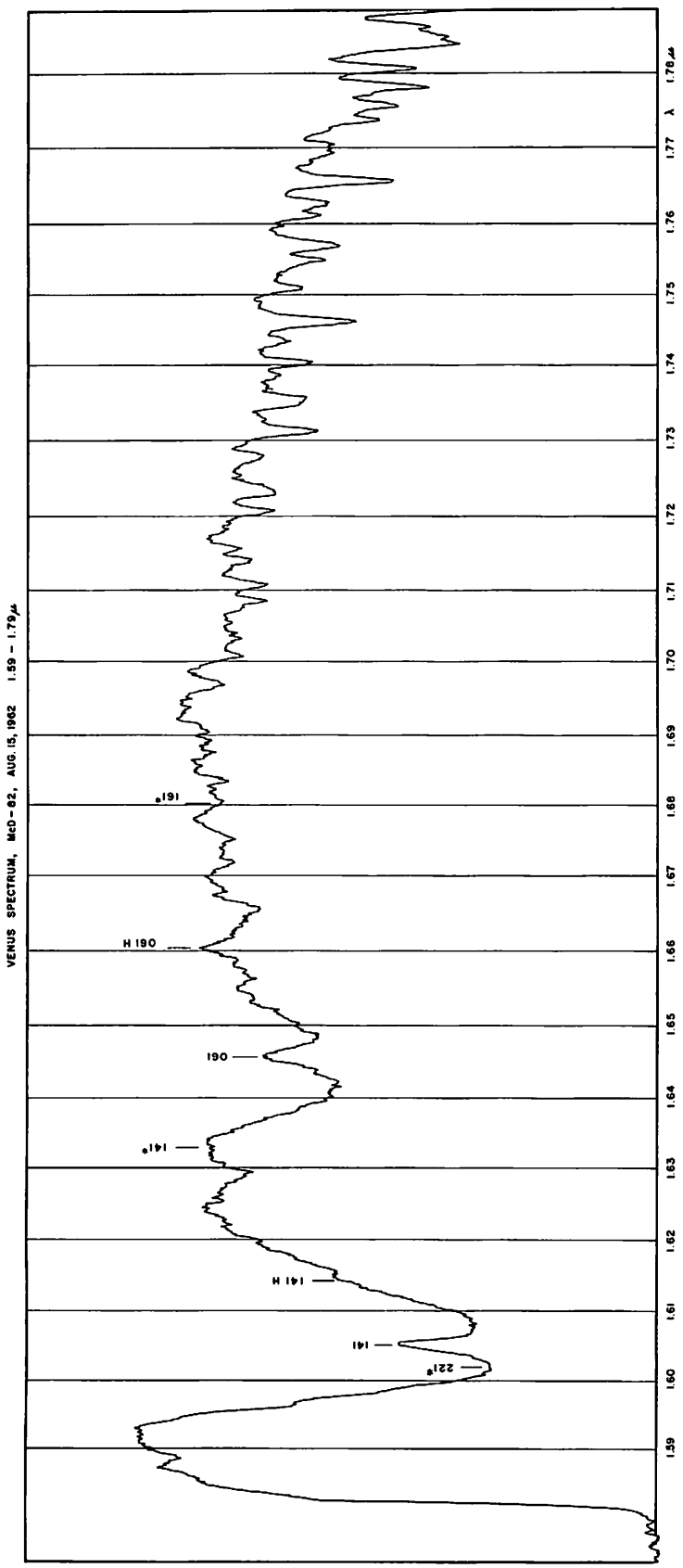

Fig. 12. Venus spectrum, 1.59-1.79μ overlapping with Figure 11*b*. Data as Figure 11*a*, but H.A. 1^h41^m-2^h22^mW. T = 24°C, H = 33%.

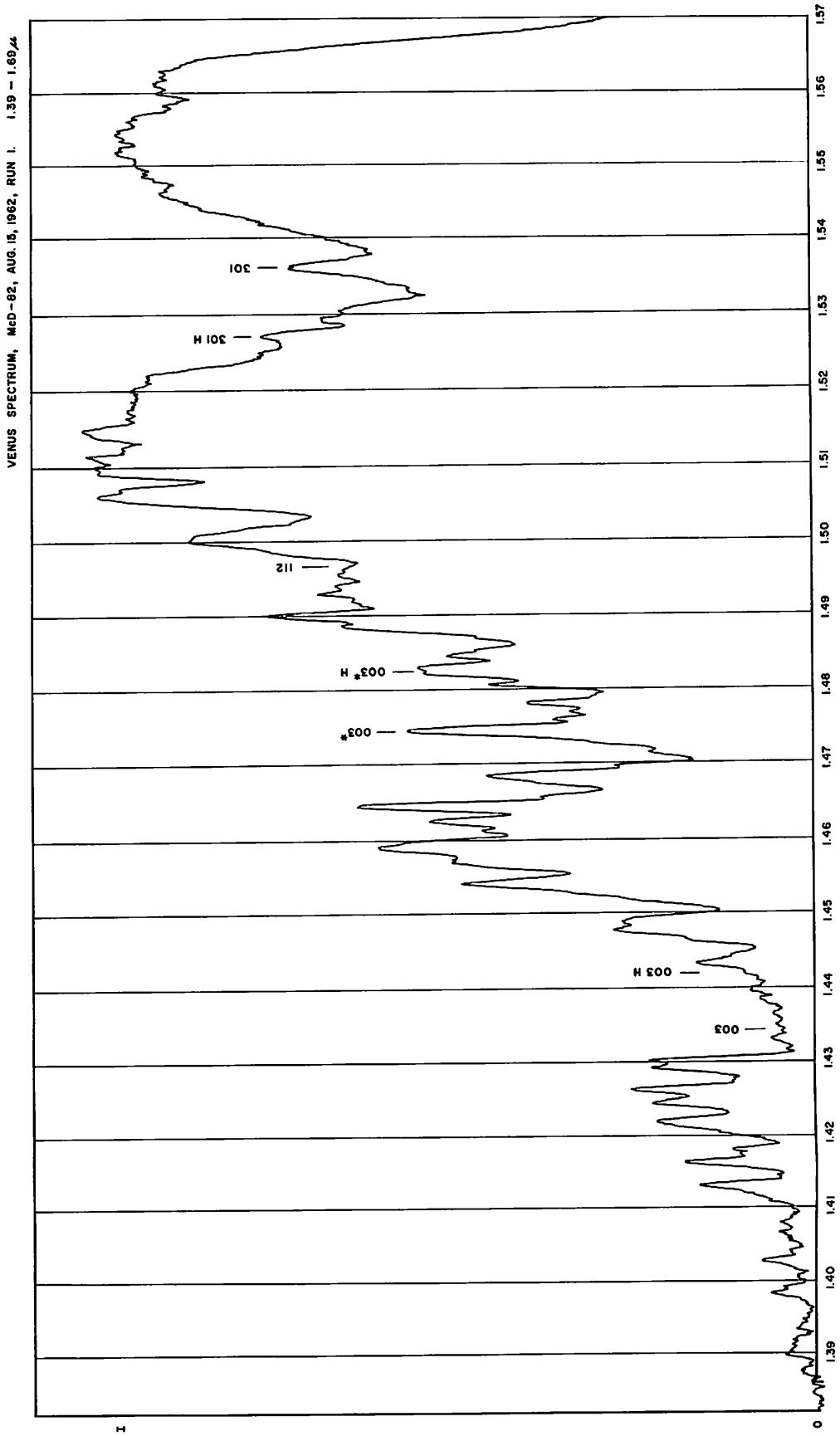

Fig. 11a. Venus spectrum, 1.39-1.69μ, Part 1. The CO_2 bands are the same as marked in Figure 2. Grating 1.6μ, filter 2540, cell width 0.10 mm, spectrometer slit 0.3 mm, $\tau = 6$ seconds. Decl. $-3°41'$, H.A. 0^h39^m-1^h40^mW. T = 24°C, H = 34%.

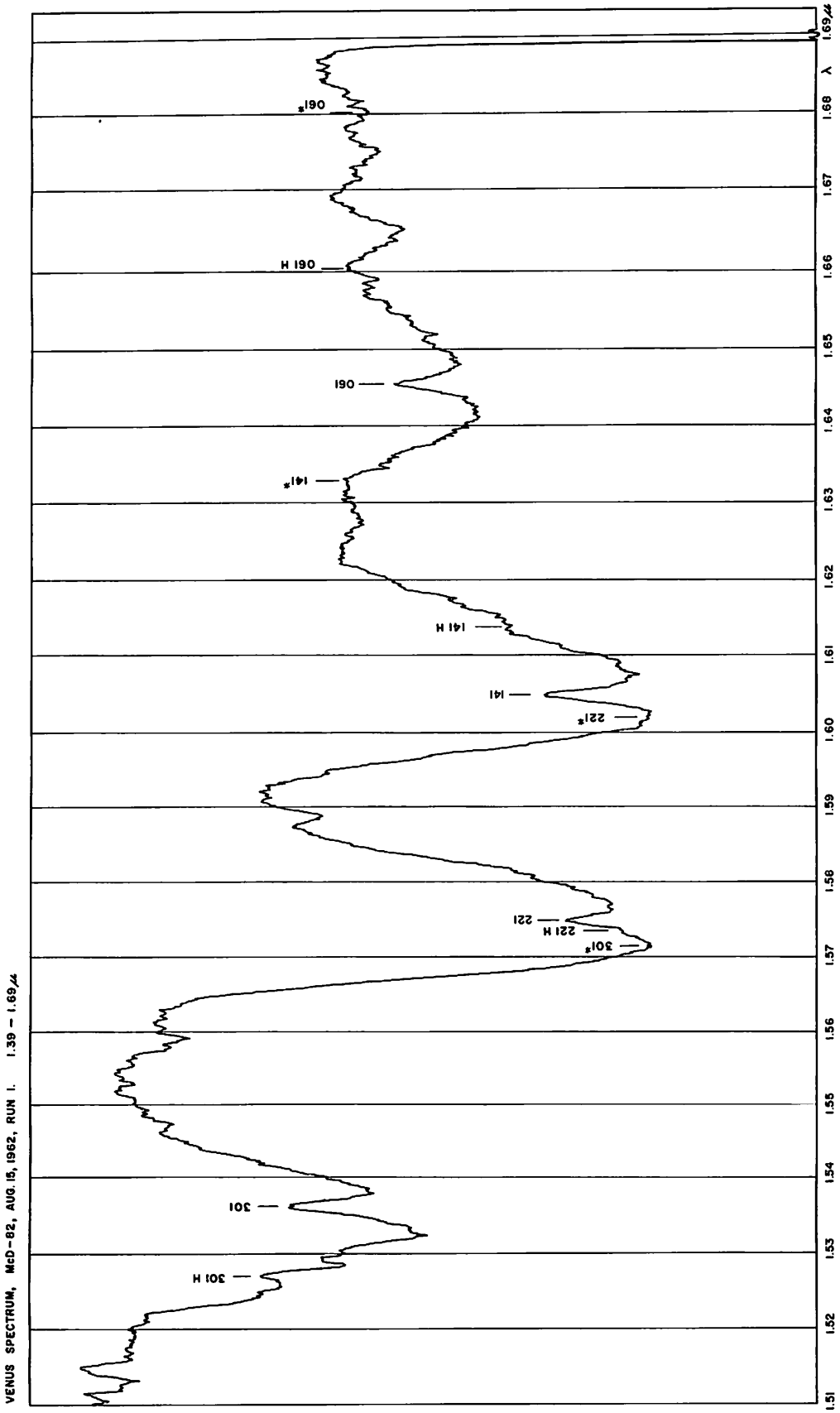

Fig. 11b. Venus spectrum, 1.39-1.69μ, Part 2.

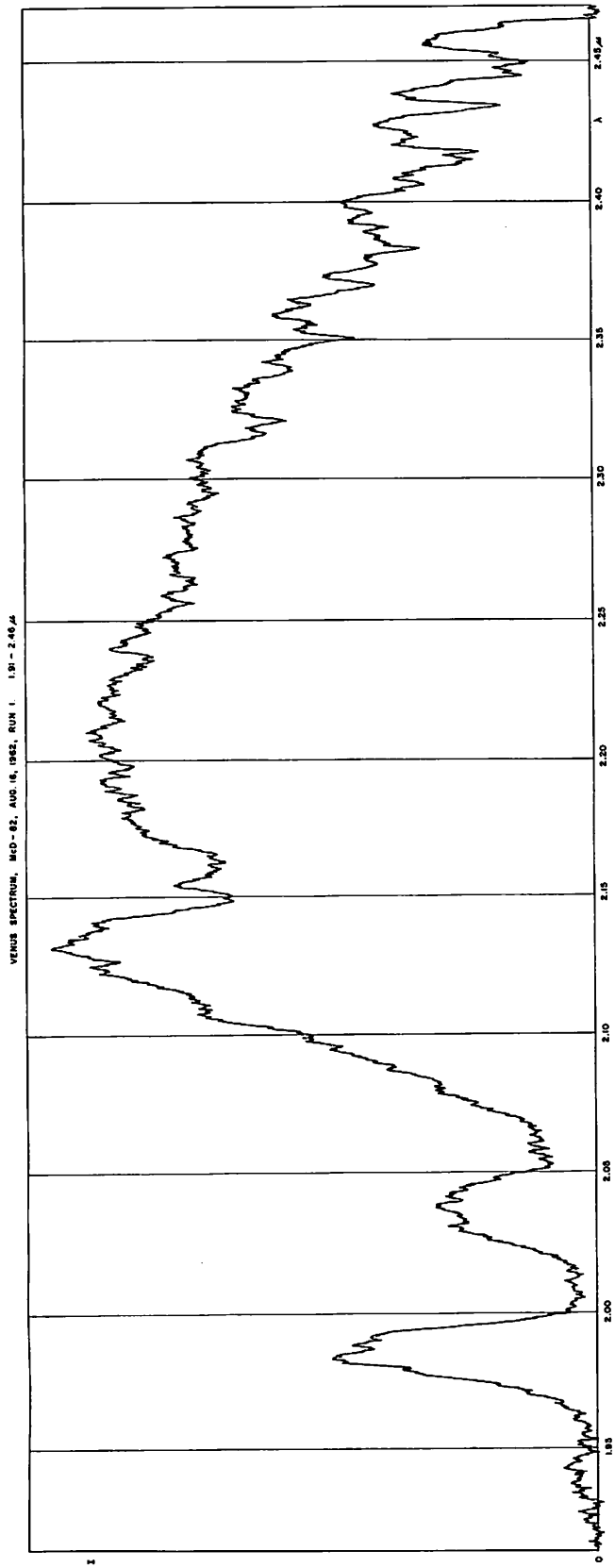

Fig. 13. Venus spectrum, 1.91-2.46μ. Grating 2μ, filter $\lambda > 1.9\mu$, cell 0.1 mm, slit 0.3 mm, $\tau = 6$ seconds. Decl. $-4°10'$, H.A. 0^h12^m-1^h02^mW. T = 23 °C, H = 38%.

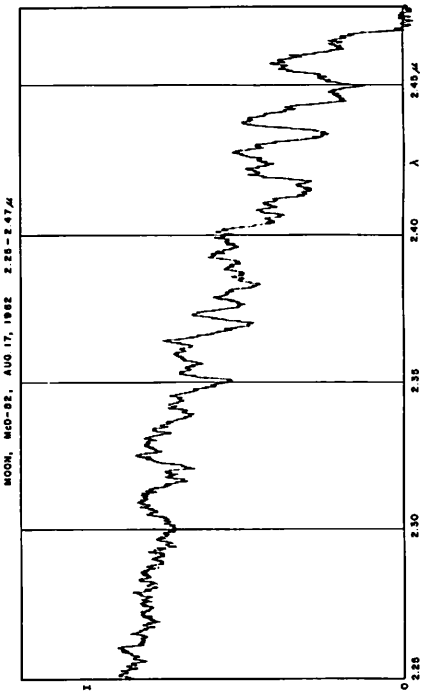

Fig. 15. Moon (terrae, out of focus), 2.25-2.47μ, grating 2μ, filter $\lambda > 1.9\mu$, cell 0.1 mm, slit 0.3 mm. $\tau = 6$ seconds. Decl. $-9°20'$, H.A. 0^h24^mW-0^h45^mW. T = 20 °C, H = 50%. (1.95-2.25μ not reproduced.)

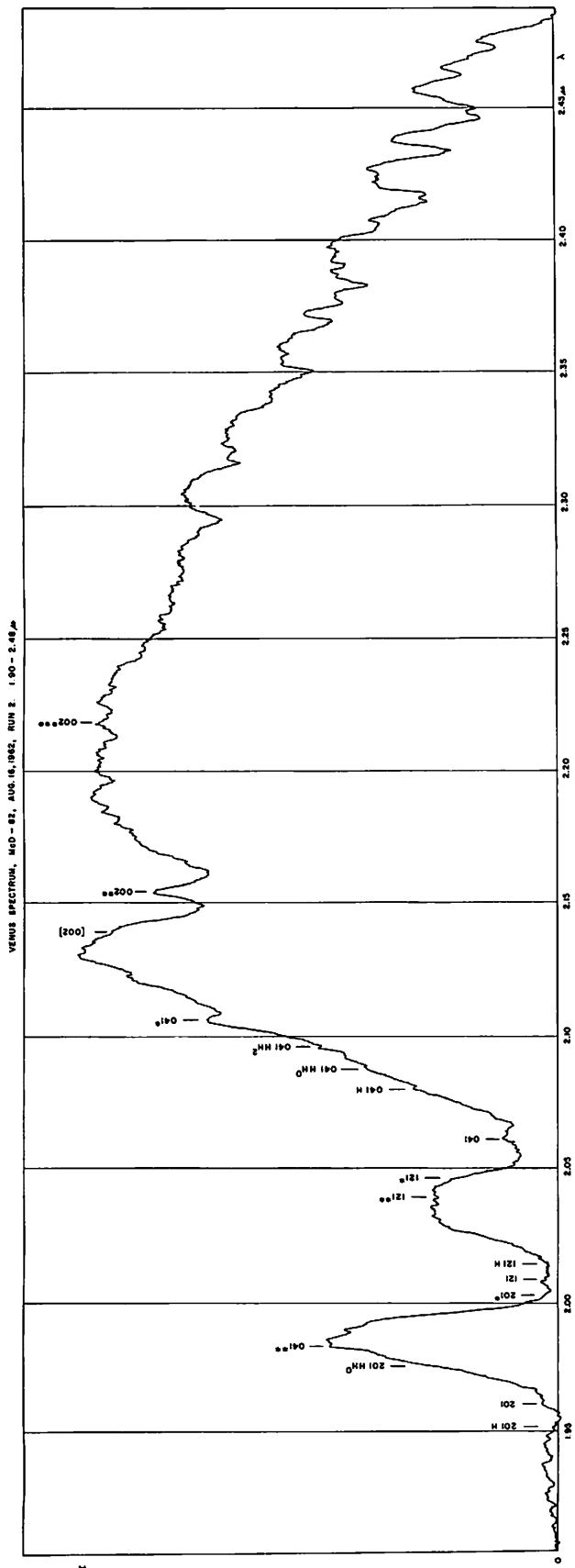

Fig. 14. Venus spectrum, 1.90-2.48μ. The CO_2 bands are the same as marked in Figure 4. Same as Figure 13, except $\tau = 12$ seconds. H.A. 1^h08^m-2^h02^mW.

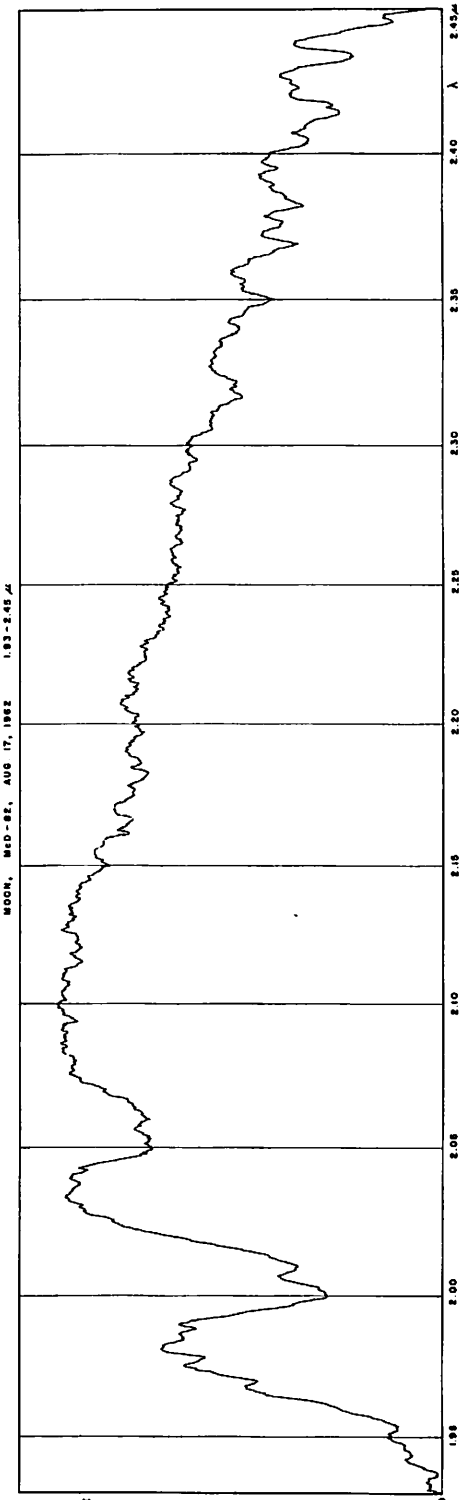

Fig. 16. Moon (terrae, out of focus), 1.93-2.45μ. Grating 2μ, filter $\lambda > 1.9\mu$, cell 0.1 mm, slit 0.3 mm. $\tau = 12$ seconds, Decl. $-9°50'$, H.A. 0^h58^mE-0^h10^mE. T = 20°C, H = 51%.

in the recorded spectrum. Stellar spectra served as additional checks on the strengths of the telluric absorptions.

The comparatively high summertime humidity of the McDonald atmosphere is apparent from the strong telluric absorptions. Additional spectral runs of Venus must be made in a dry winter atmosphere. Nevertheless, the present McDonald spectra add information on the wavelengths of the new bands, and are therefore reproduced in full.

Figures 8 and 9 show two consecutive runs on the region 1.18-1.35μ. For the sake of completeness an earlier microphotometer tracing of the three bands between 1.0 and 1.1μ is added in Figure 10. This tracing also clarifies the characteristic band shape for the Σ-Σ transitions in the IR tracings, such as the depths and widths of the *R* and *P* branches and the position of the origin, the point indicated in the tracings.

Comparison of Figures 8 and 1 shows that the added resolution has clarified, e.g., the location of the band heads near 1.23μ. A small difference exists in the shapes of the (401) band where it merges with the telluric O_2 band at 1.268μ. An earlier record with the same resolution, but higher noise level than Figure 1*a* was available; the relevant part is reproduced in Figure 1*b*. On this record the (401) band has intermediate strength.

Figures 11 and 12 cover the region 1.39-1.79μ. The structure of slopes of the strong CO_2 bands is now more clearly brought out, allowing more certain identification (Sec. 4). The numerous features from 1.68-1.79μ are telluric.

The region 1.9-2.5μ was recorded in two consecutive runs on August 16, 1962, with different time constants, and reproduced in Figures 13 and 14. The 12-second time constant (Fig. 14) shows the CO_2 bands more firmly. The lunar comparison spectra obtained with the same time constants and slit widths are reproduced in Figures 15 and 16. They are rather noisy because of the low surface brightness of the moon but they show no appreciable differences from Venus at $\lambda > 2.20\mu$. It is found that the three CO_2 bands marked in this region by Gebbie *et al.* (1962) are not real.

4. Interpretation and Laboratory Spectra

Several prominent absorption bands in the Venus spectrum have been known to be due to CO_2. They arise from the ground state and contain the *odd* overtones of ν_3, namely ν_3, $3\nu_3$ and $5\nu_3$, with various combinations of ν_1 and ν_2 in Fermi resonance leading to the formation of diades, triades, tetrades, pentades, etc. These transitions are of the type $\Sigma_u^+ \leftarrow \Sigma_g^+$, not involving a change in the azimuthal quantum number *l*, and have two branches, *R* and *P*, which are resolved in our spectra, though the finer rotational structure is not. In addition, there are much weaker permitted transitions from the ground state of the type $\Pi_u \leftarrow \Sigma_g^+$, involving the *even* overtones of ν_3 and such combinations of ν_1 and ν_2 that $(v_2 + v_3)$ is odd; even combinations of $(v_2 + v_3)$ are forbidden. These transitions involve a change by 1 of the azimuthal quantum number and cause the presence of a Q branch, which on our spectra makes the band look like a narrow feature with a pointed minimum.

A list of the permitted transitions from the ground state was constructed on the basis of the energy diagram given by Herzberg and Herzberg (1953, p. 1041). Comparison of this list with the very detailed laboratory investigations by Courtoy (1957, 1959) showed that additional bands must be present in the Venus spectrum arising from the $\Pi_u(01^10)$ level and possibly even the higher levels, $\Sigma_g^+ 02^00$, $\Delta_g 02^20$, and $\Sigma_g^+ 10^00$. These bands, conveniently called the "hot" and "doubly-hot" bands, are of interest in connection with a possible determination of the temperature of the Venus atmosphere.

Accordingly, we have collected in Table 1 all transitions for $\lambda < 2.5\mu$ that seemed relevant or promising, including the strongest isotopic bands of $^{13}CO_2$ and $^{12}C^{18}O^{16}O$. The latter were taken from the laboratory studies by Courtoy (1959), as were the wavelengths of all other relevant bands listed by him. Some permitted bands, such as 212, were dropped when no evidence for their presence was found in Venus or the laboratory.

The complexity of the CO_2 spectrum is sufficient to prevent the classification of the weaker bands without laboratory spectra showing the rotational structure. In particular, the hot bands and the isotopic bands appear as satellites of the principal bands arising from the ground state of the $^{12}CO_2$ molecule, often present as disturbing features in the wings. Thus $\nu_2 + 3\nu_3 - \nu_2$ at $\lambda = 1.442\mu$ occurs in the *P* branch of $3\nu_3$; and the triade 201, 121, 041 at $\lambda = 1.961$, 2.009, and 2.060μ has the companion bands $2\nu_1 + \nu_2 + \nu_3 - \nu_2$, $\nu_1 + 3\nu_2 + \nu_3 - \nu_2$, and $5\nu_2 + \nu_3 - \nu_2$, at $\lambda = 1.952\mu$, 2.014μ, and 2.080μ, respectively. To bring out this correspondence we have used the symbols 201H, 121H, and 041H for these companions in Table 1 and in the figures. Doubly-hot companions are indicated by HH^0 or

HH^2, depending on the quantum number l of the lower state.

The isotopic bands are marked by asterisks. Since the $^{12}C/^{13}C$ ratio on the Earth is 89, and the $^{16}O/^{18}O$ ratio about 500, a single asterisk was used for ^{13}C isotopes and a double asterisk for ^{18}O isotopes. The equivalent intensity of single-asterisk bands may therefore be down by two orders of magnitude, the intensity of the double asterisk bands by nearly three. On the assumption that the strength of the hot bands on Venus is down by one order of magnitude or more, the combination *H was retained, but not **H or *HH.

As Courtoy has found and as may be seen from Table 1, the positions of the ^{18}O isotopic bands with respect to the ^{16}O bands are irregular, unlike the positions of the ^{13}C or $^{18}O^{18}O$ isotopes where nearly constant ratios with the wavelengths of the principal bands are maintained.

The symbols in the last column of Table 1 have been transferred to the figures where this appeared warranted. It is found that the Venus absorption can be satisfactorily accounted for by the permitted transitions listed in Table 1 with one major exception, the band at 2.15μ. In addition, a few minor features remain unexplained. Both the 2.15μ band and the minor features are present in the laboratory spectra of CO_2, and are therefore attributed to CO_2.

No permitted $^{12}CO_2$ or $^{13}CO_2$ transition appears to fit the $\lambda = 2.15\mu$ band. Accordingly, the possibility of its being a pressure-induced dipole or a quadrupole transition of $^{12}CO_2$ was examined. The forbidden $2\nu_3$ transition from the ground state fits the observed position $\nu_0 = 4643 \pm 5$ rather closely, but not precisely, the computed position being $\nu_0 = 4673$. Dr. Herzberg suggested to the writer that the observed band may rather be identified as the $^{12}C^{18}O^{16}O$ isotopic $2\nu_3$ band, which is permitted because of the asymmetry of the molecule. The writer had already estimated that the observed band was roughly 10^3 times weaker than expected from a fully permitted $2\nu_3$ band. This ratio is of the same order of magnitude as the $^{18}O/^{16}O$ ratio. Dr. Herzberg has computed the position of this isotopic band at $\nu_0 = 4639$, in full accord with the observations. This identification is of special interest because the unhampered observation of what would be normally a very weak isotopic companion is made possible because the principal band is forbidden and a permitted $2\nu_3$ transition very strong.

The minor CO_2 features in the 1.6μ region will be examined in greater detail in future laboratory investigations. It will also be attempted to resolve the rotational structure of the isotopic $2\nu_3$ band to settle the identification.

The Venus spectra give information on (a) the the CO_2 abundance on Venus; (b) the $^{13}C/^{12}C$ ratio; (c) the $^{18}O/^{16}O$ ratio; (d) the hot bands.

(a) The CO_2 abundance is found from the relation between Venus band strength and laboratory band strength. The discussion is limited to bands of the type $\Sigma_g^+ \rightarrow \Sigma_u^+$ (i.e., the ν_3, $3\nu_3$, and $5\nu_3$ series) in the spectral region 1.20-1.66μ for which the Venus photometry (Figs. 1 and 2) is satisfactory and the range of available band intensities suitable. A laboratory spectrum similar to that reproduced in Figure 17 was used for the comparison. The equivalent widths of twelve $^{12}CO_2$ bands and one $^{13}CO_2$ band were determined from planimeter measures on the original tracings, with allowance for the mean ordinate of the interpolated continuum at each absorption band. The (401) Venus band was measured on the trace of Figure 1*b* for the reasons stated earlier.

Equivalent widths in different spectral regions are not directly comparable. The laboratory spectra reproduced show that the widths of the CO_2 bands increase from about 0.01μ at $\lambda = 1.2\mu$ to 0.035μ at $\lambda = 2.15\mu$. This increase is in accord with theory. The band width is determined by the intensity distribution of the rotational lines, which will be similar for the various $\Sigma_u \leftarrow \Sigma_g$ transitions. Therefore the band widths are essentially constant when measured in wave numbers, $\Delta\nu$, and will vary as λ^2 when measured in $\Delta\lambda$. Division of the equivalent widths by λ^2 will therefore make them comparable throughout the spectrum.

The equivalent widths of the CO_2 bands, in Angstrom units and divided by λ^2, are recorded in Table 2 and plotted in Figure 22. It is noted that the strong bands are stronger in the laboratory spectrum while the reverse is true for the weaker bands. This is explained by the reduced penetration into the Venus atmosphere with increasing band strength. The limiting penetration for very weak bands may be used to define the observable depth of the Venus atmosphere. The curve must pass through the origin and is presumably not tangent to the y-axis since the opacity of the Venus atmosphere in red and infrared light between the CO_2 bands is not due to Rayleigh scattering, but to a diffuse cloud of particles, so that, as seen in the weakest bands, the cloud layer on Venus limits the penetration. The slope of the curve

TABLE 1

CO_2 BANDS OBSERVED IN VENUS AND LABORATORY

(λ and ν_0 of band origin)

$\lambda(\mu_0)$ (vac.)	λ(Head) (Air)	ν_0	Transition*	Symbol Used In Figures
0.7165	0.7158	13957	12^05	125
0.7828	0.7820	12774.7	10^05	105
0.7891	0.7883	12672.3	02^05	025
0.8698	0.8689	11496.4	00^05	005
0.8749	0.8736	11430	01^15-01^10	005H
0.9267:		10790.4:	14^03	143
0.9244:		10817.2:	22^03	223
1.0383	1.0362	9631.4	20^03	203
1.0508	1.0488	9517.0	12^03	123
1.0651	1.0627	9389.0	04^03	043
1.2055	1.2030	8294.0	10^03	103
1.2082	1.2055	8276.8	11^13-01^10	103H
1.2206	1.2177	8192.6	02^03	023
1.2291	1.2262	8136.0	03^13-01^10	023H
1.2364		8089.0	$10^03(^{13}C)$	103*
1.2530		7981.2	$02^03(^{13}C)$	023*
1.2606		7932.9	21^12	212
1.2625		7920.5	40^01	401
1.2929		7734.3	32^01	321
1.294		7730	33^11-01^10	321H
1.3116		7624.0	25^11-01^10	241H
1.3169		7593.5	24^01	241
1.3367		7481.3	$24^01(^{13}C)$	241*
1.3404		7460.4	16^01	161
1.3729		7284.0	08^01	081
1.4342		6972.5	00^03	003
1.4420		6935.0	01^13-01^10	003H
1.444		6925	$00^03(^{18}O)$	003**
1.4749		6780.1	$00^03(^{13}C)$	003*
1.4826		6745.0	01^13-$01^10(^{13}C)$	003*H
1.497		6681	11^12	112
1.507:		6636:	03^12	032
1.5299		6536.4	31^11-01^10	301H
1.5377		6503.0	301	301
1.5714		6363.6	$301(^{13}C)$	301*
1.5733		6356.2	23^11-01^10	221H
1.5753		6347.8	22^01	221
1.6021		6241.9	$22^01(^{13}C)$	221*
1.6057		6227.9	14^01	141
1.6139		6196.1	15^11-01^10	141H
1.6341		6119.6	$14^01(^{13}C)$	141*
1.6458		6075.9	06^01	061
1.6609		6020.8	07^11-01^10	061H
1.6802		5951.5	$06^01(^{13}C)$	061*
1.8812		5315.7	01^12	012
1.8900		5291.1	02^22-01^10	012H
1.9348		5168.6	$01^12(^{13}C)$	012*
1.9457		5139.4	22^21-02^20	$201HH^2$
1.9519		5123.2	21^11-01^10	201H
1.9609		5099.6	20^01	201
1.9754		5062.4	22^01-02^00	$201HH^0$
1.9831		5042.5	$04^01(^{18}O)$	041**
2.0035		4991.3	$20^01(^{13}C)$	201*
2.0089		4977.8	12^01	121

TABLE 1. CONTINUED

$\lambda(\mu_0)$ (vac.)	λ(Head) (Air)	ν_0	Transition*	Symbol Used In Figures
2.0140		4965.3	$13^{1}1\text{-}01^{1}0$	121H
2.0388		4904.8	$20^{0}1(^{18}O)$	121**
2.0461		4887.3	$12^{0}1(^{13}C)$	121*
2.0603		4853.6	$04^{0}1$	041
2.0800		4807.7	$05^{1}1\text{-}01^{1}0$	041H
2.0872		4791.2	$20^{0}1(^{18}O)$	201**
2.0875		4790.5	$06^{0}1\text{-}02^{0}0$	$041HH^{0}$
2.0971		4768.5	$06^{2}1\text{-}02^{2}0$	$041HH^{2}$
2.1061		4748.0	$04^{0}1(^{13}C)$	041*
2.1238		4708.5	$05^{1}1\text{-}01^{1}0(^{13}C)$	041*H
2.1341		4685.7	$06^{0}1\text{-}02^{0}0(^{13}C)$	$041*HH^{0}$
2.1397		4673.6	$06^{2}1\text{-}02^{2}0(^{13}C)$	$041*HH^{2}$
2.140		4673	$[00^{0}2]$	[002]
2.1556		4639	$00^{0}2(^{18}O)$	002**
2.220		4505	$00^{0}2(^{18}O,^{13}C)$	002***
			$01^{1}2\text{-}01^{1}0(^{18}O)$	002**H

*From ground state Σ_g^+ $00^{0}0$ unless stated otherwise.

TABLE 2

EQUIVALENT WIDTHS IN WAVELENGTH AND FREQUENCY UNITS, OF CO_2 BANDS IN VENUS AND LABORATORY SPECTRA

Band	EW(Venus) (A)	EW/λ^2 (A/μ^2)	EW(Lab.) (A)	EW/λ^2 (A/μ^2)
103	42	29	43	30
023	30.3	20	33	22
401	6.7	4.2	1	0.7
321	16	9.6	8	5
241	27	15.6	18	10.4
161	15	8.4	5	2.8
003	129	63	204	99
003*	34	16	33	15
301	61	26	87	37
221	122	49	180	72
141	154	60	235	91
061	72.5	27	103	38
002**	77	16.5	59	12.7

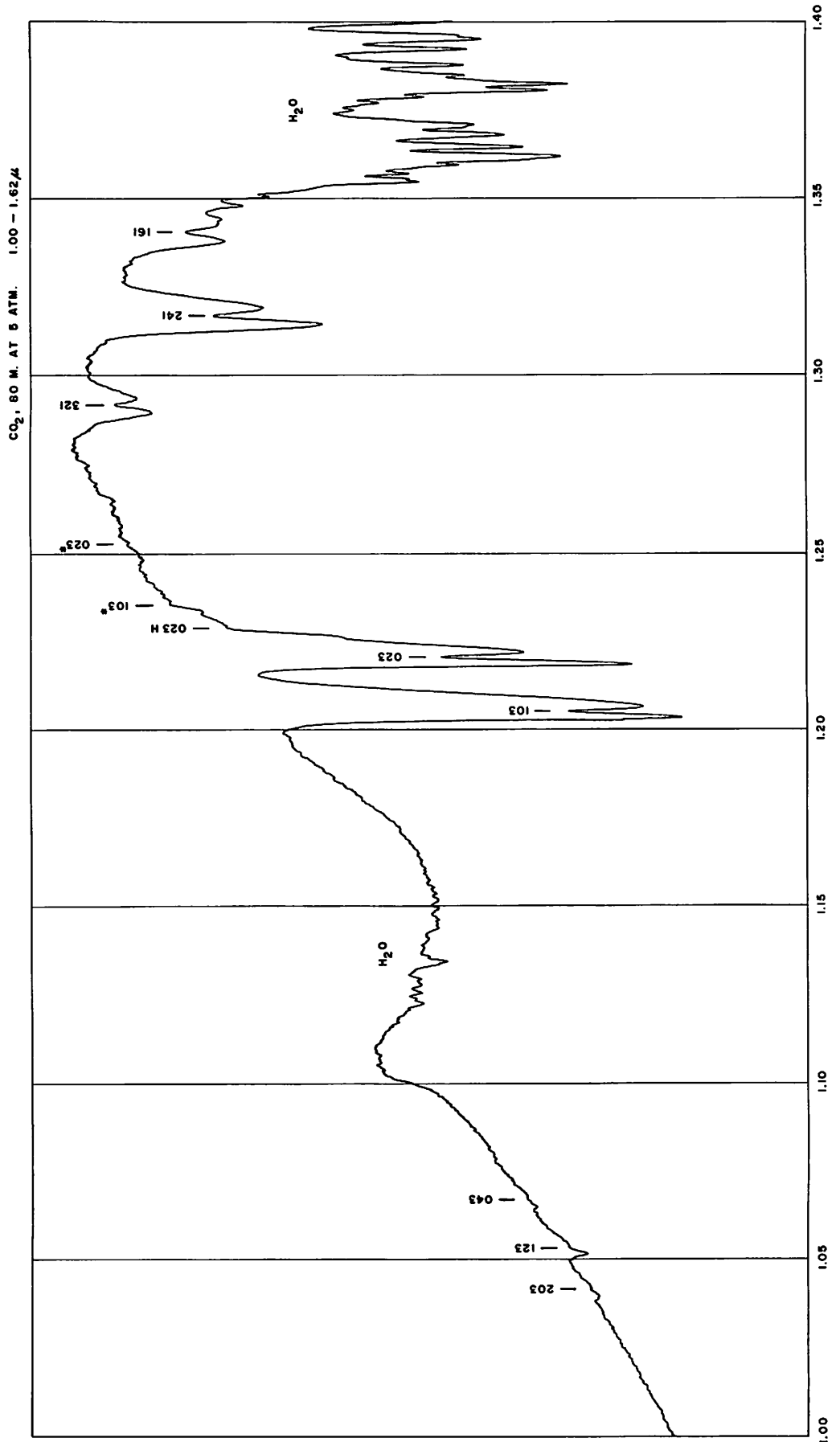

Fig. 17a. CO_2 spectrum, 80 meter path at 5 atm., 1.00-1.40μ. Grating 1.6μ, filter 2540, cell 0.25 mm, slit 0.25 mm, $\tau = 2.5$ sec.

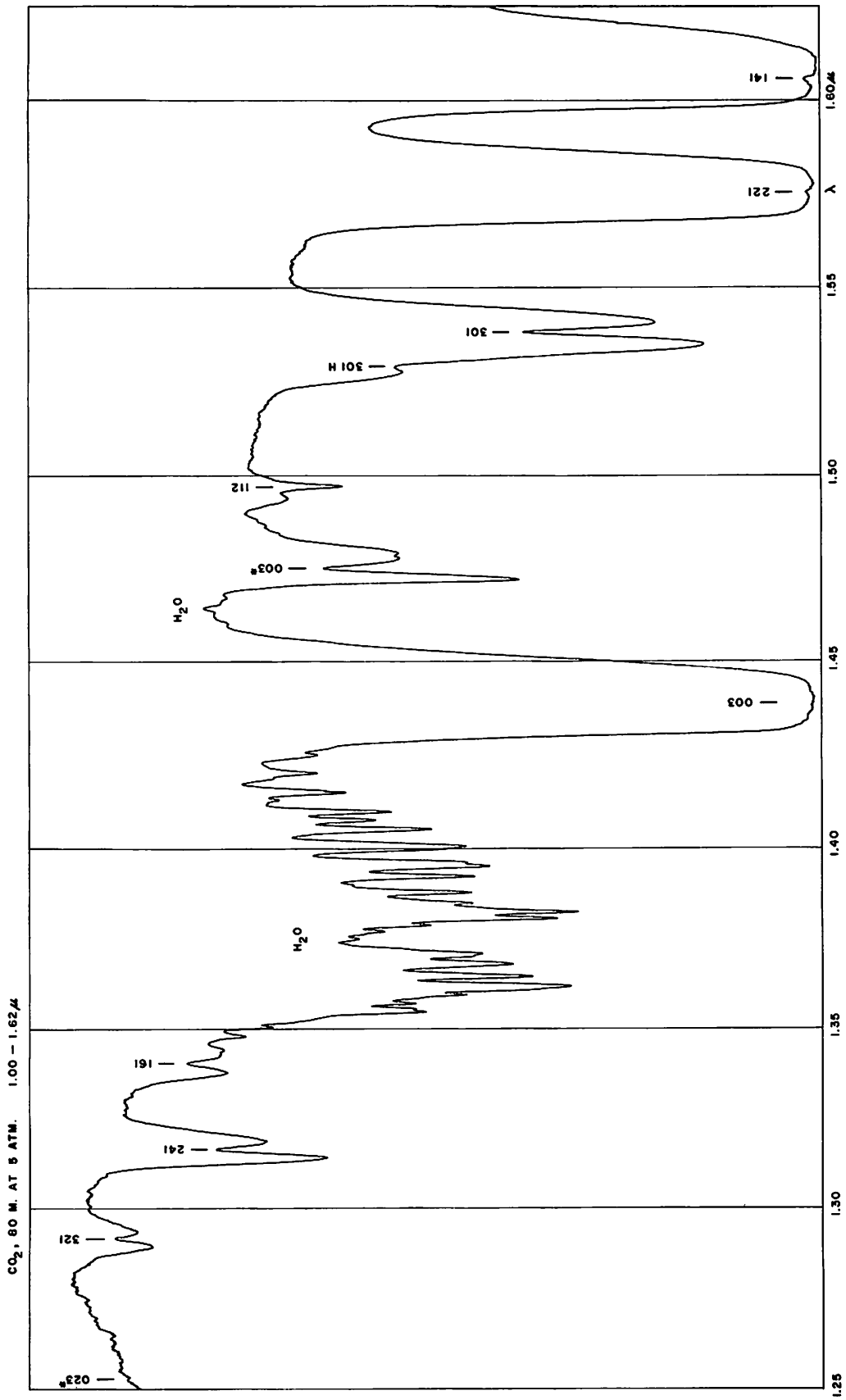

Fig 17b. CO_2 spectrum, 80 meter path at 5 atm., 1.25-1.62μ. Grating 1.6μ, filter 2540, cell 0.25 mm, slit 0.25 mm, $\tau = 2.5$ sec.

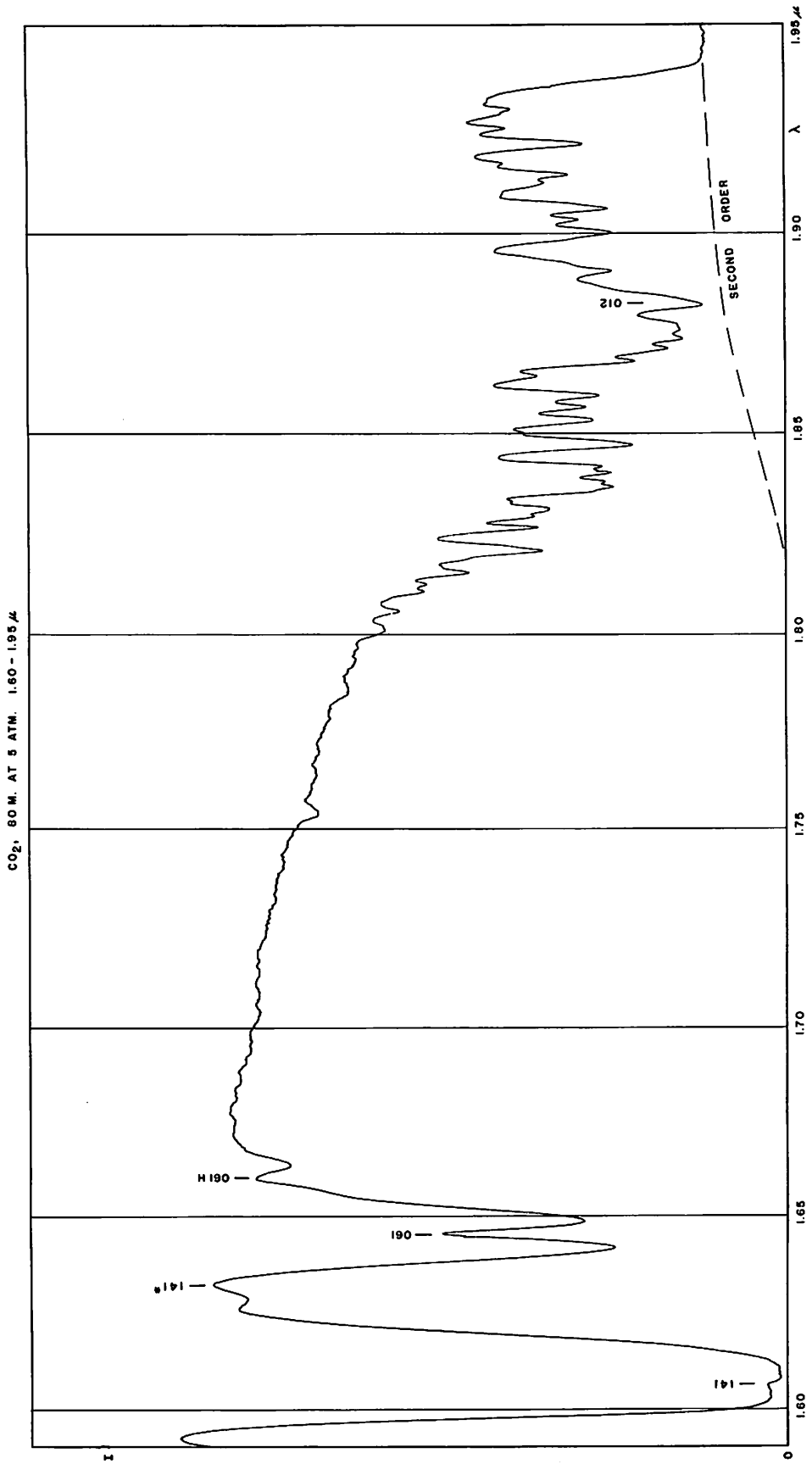

Fig. 17c. As 17*a,b*, 1.60-1.95μ. The zero level 1.84-1.95μ is raised by second-order 0.92-0.97μ passing the 2540 filter.

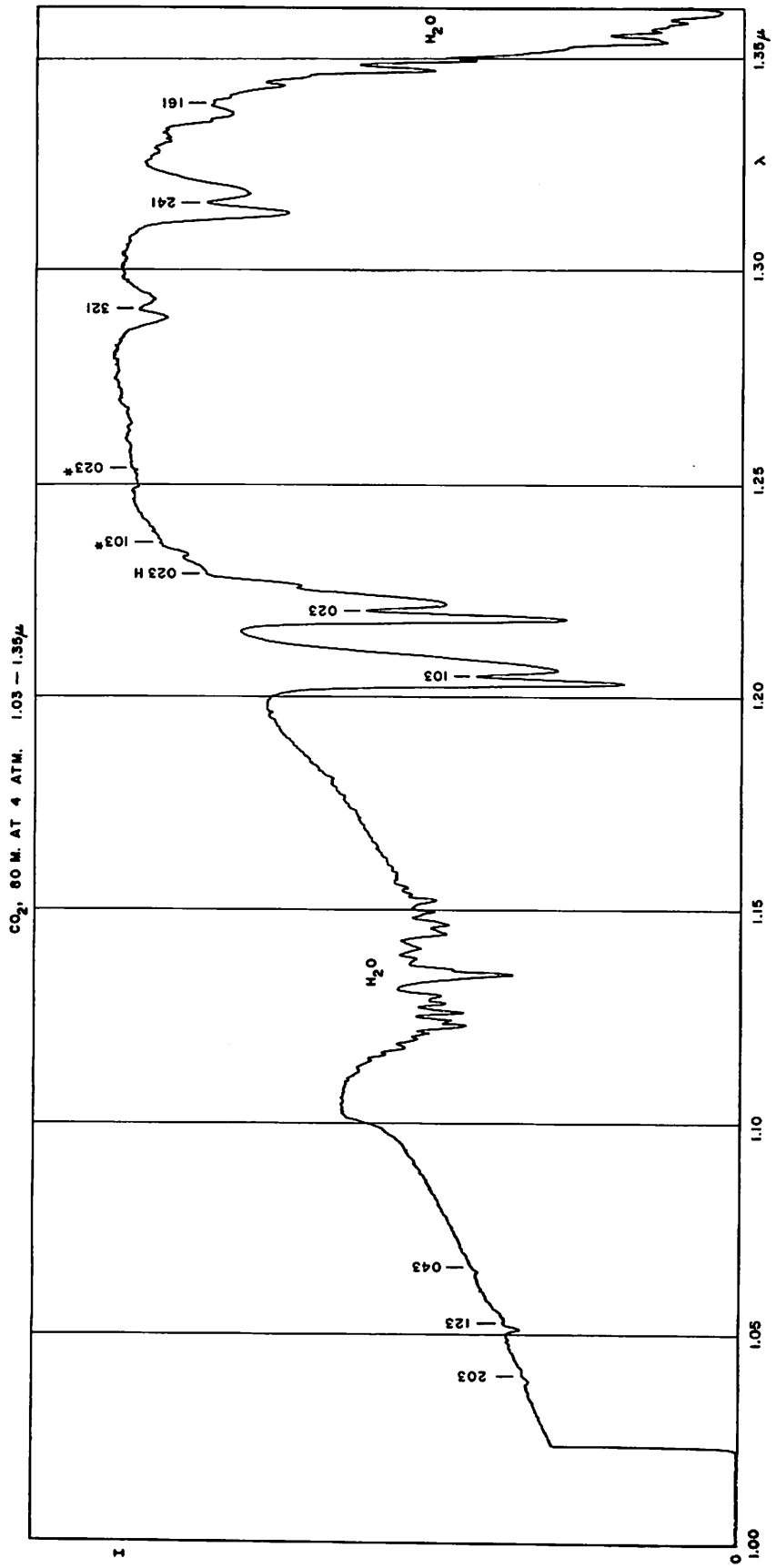

Fig. 18a. CO_2 spectrum, 80 meters at 4 atm., 1.03-1.35μ. Grating 1.6μ, filter 2540, cell 0.25 mm, slit 0.25 mm, $\tau = 1.2$ sec.

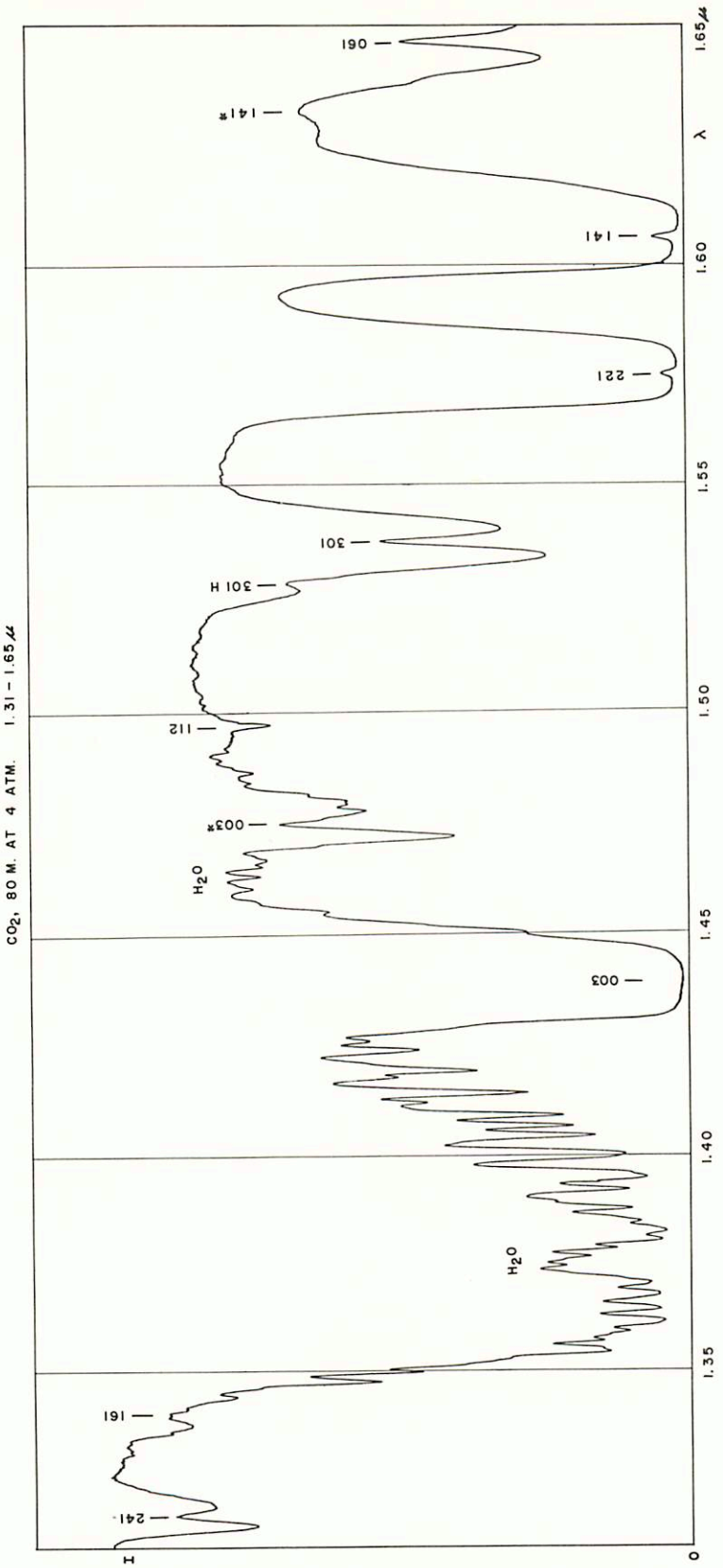

Fig. 18b. As 18*a*, 1.31-1.65μ

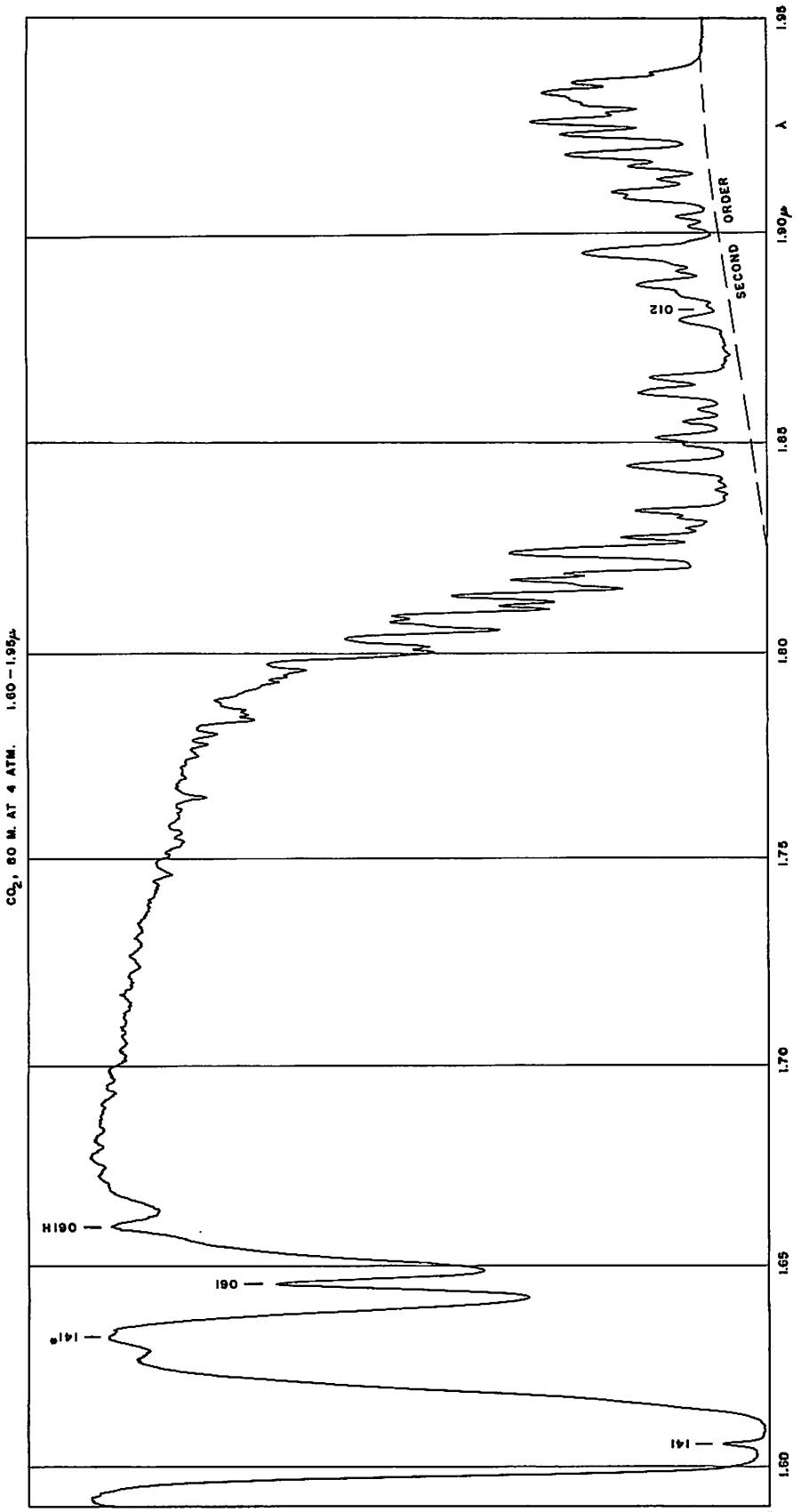

Fig. 18c. As 18*a*, 1.60-1.95μ. Second-order spectrum as in Figure 17*c*.

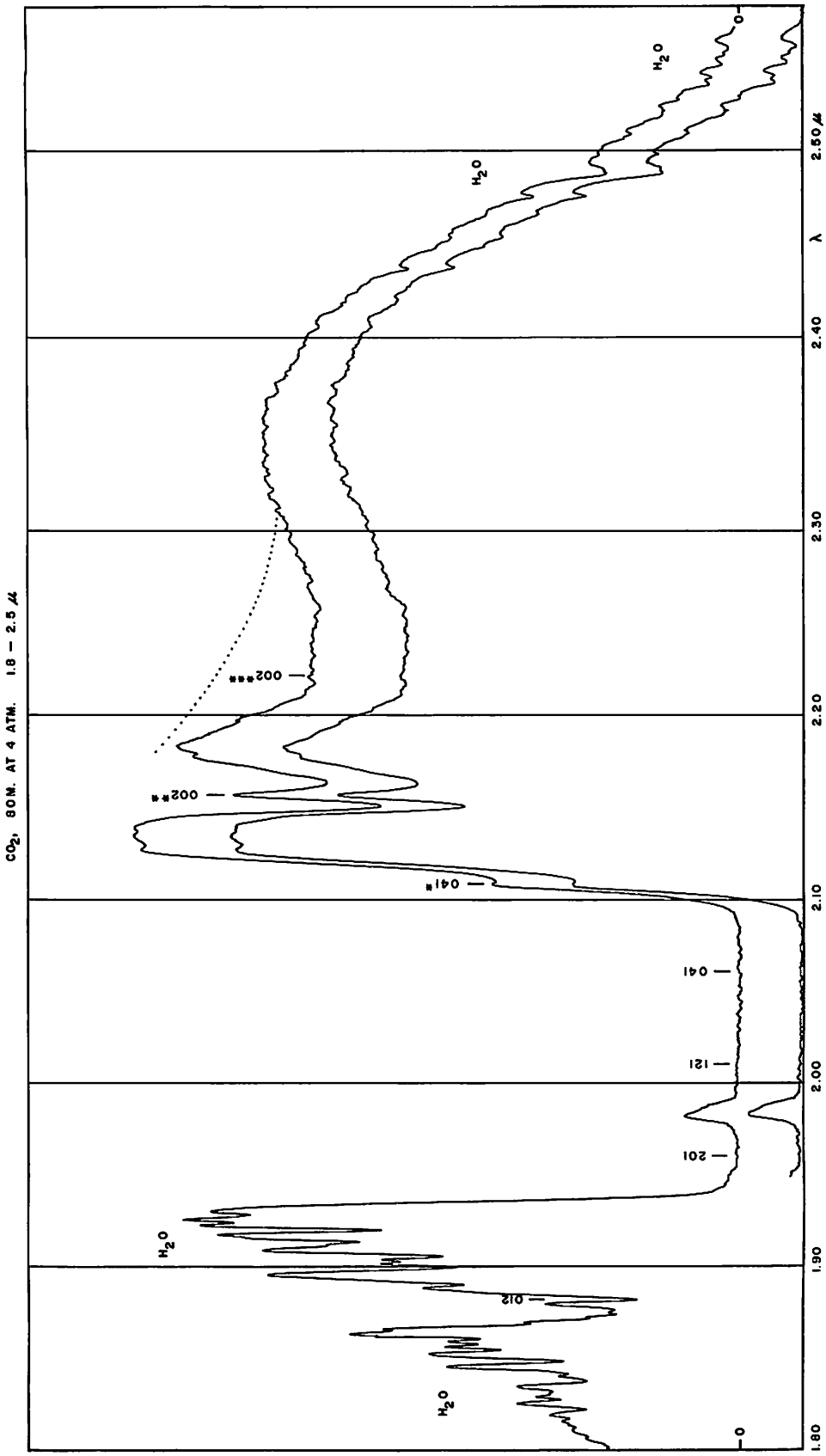

Fig. 19. CO_2 spectrum, 80 meter path at 4 atm., 1.8-2.5μ. Grating 2μ, filter $\lambda > 1.8\mu$, cell 0.25 mm, slit 0.25 mm, $\tau = 2.5$ seconds. The shallow dip 2.18-2.3μ is not duplicated in two blank runs whose course is indicated by dots (cf. also Fig 20). This dip resembles that in the Venus spectrum (cf. Fig. 4), but appears absent in Figure 20. Further tests will be made to determine whether this effect is instrumental.

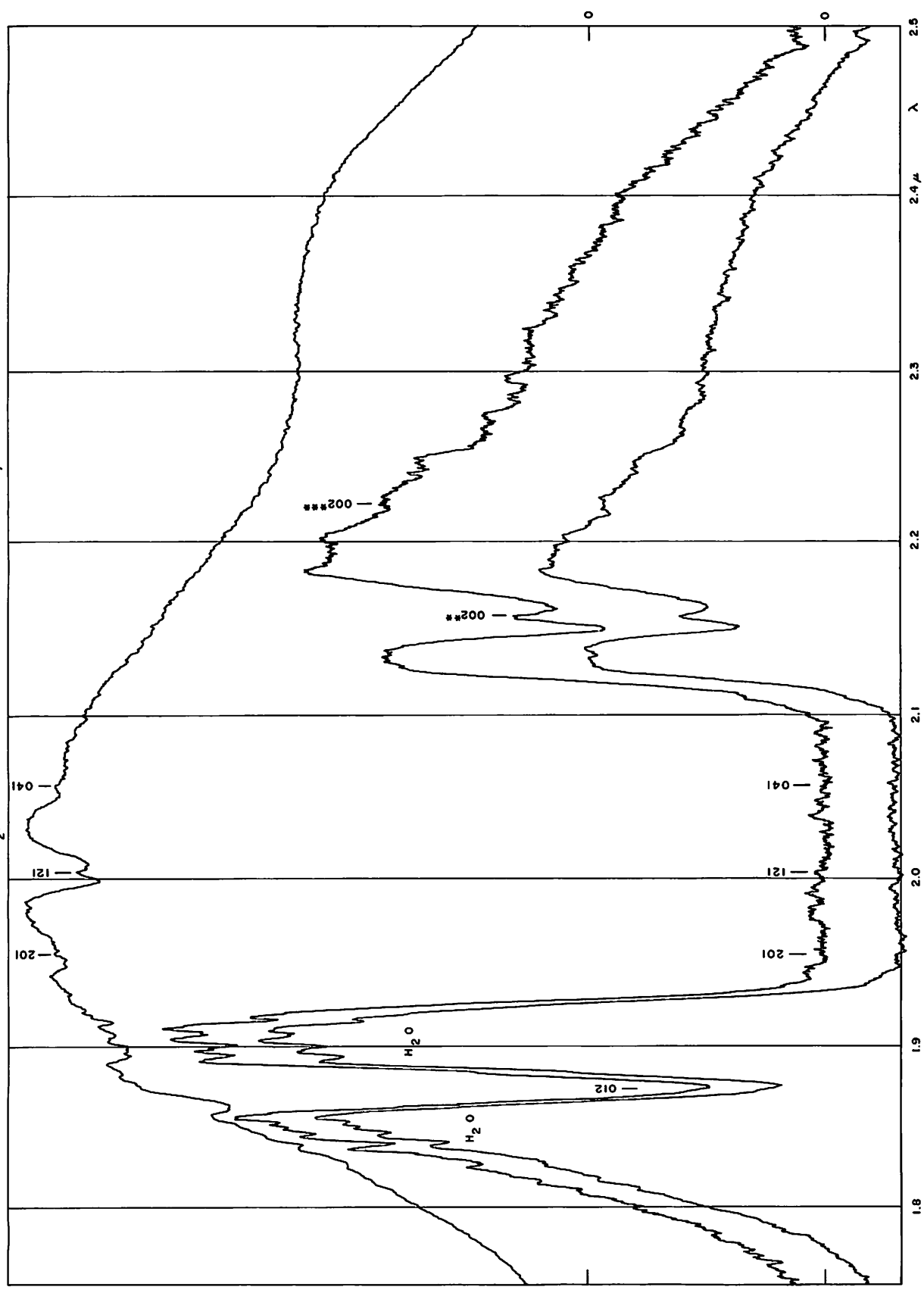

Fig. 20. CO_2 spectrum, 80 meter path at 17 atm., 1.8-2.5μ. Grating 2μ, filter $\lambda > 1.8\mu$, cell 0.25 mm, slit 0.28 mm, $\tau = 6$ seconds. The H_2O and CO_2 absorptions contributed by the 4½ meter air path in the laboratory and the spectrometer are shown in the upper curve. The zero intensity levels are indicated in the margins.

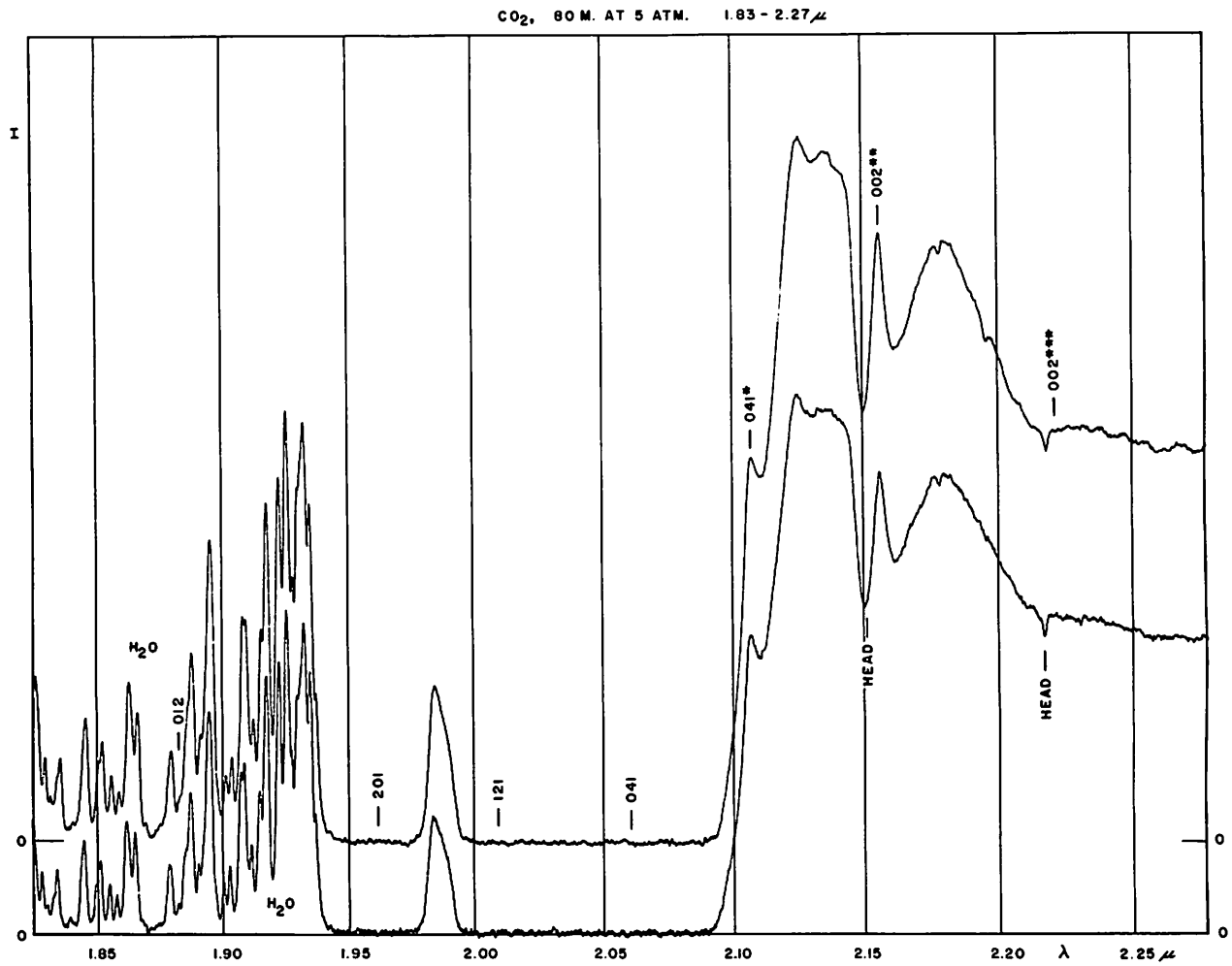

Fig. 21. CO_2 spectrum, 80 meter path at 5 atm., 1.83-2.27μ. Grating 1.6μ, filter $\lambda > 1.8\mu$, cell 0.25 mm, slit 0.35 mm, $\tau =$ 1.2 seconds. Resolution somewhat improved over Figure 19.

near the origin is about 6, so that for weak bands the Venus spectrum corresponds to about 6 x 80 meters x 4 atm. of CO_2 or about 2 km atm. of CO_2. Since the line absorptions must add linearly for very weak bands, this result should be independent of pressure. However, since the strength of the CO_2 absorption on Venus is variable, both with phase and from day to day, and even region to region on the planet (Kuiper, 1952), the amount of CO_2 found only applies to the date of observation.

The amount of water vapor shown in Figure 17 is comparatively small. Figure 18 supplements Figure 17 in showing the blending resulting from an increased amount of vapor, comparable to the amount present in the atmosphere under average dry observing conditions, i.e., somewhat better than shown in Figures 1-6.

(b) Considerable interest attaches to the abundance ratio $^{13}C/^{12}C$ on Venus. On the Earth this ratio is 1/89; in some R stars it reaches a value as high as 1/5, and in some N stars ½ (McKellar, 1960). The equilibrium ratio attained if the carbon-nitrogen cycle of nuclear energy production were operative to the exclusion of other processes is ¼ if the H abundance is greater than the C abundance (Caughlan and Fowler, 1962). Fowler, Greenstein, and Hoyle (1962) attribute the terrestrial isotope ratio to a non-equilibrium nuclear process occurring in the T Tauri stage of the solar nebula. On this basis the isotope ratio on Venus might be higher, owing to the greater proximity to the Sun.

The $3\nu_3$ isotopic band at $\lambda = 1.47\mu$ is the strongest available for measurement and was included in Table 2 and Figure 22. Laboratory spectra with increased pathlengths and improved definition will allow an extension of the discussion to other isotopic bands shown in Venus, particularly 103, 023, 061, and 041.

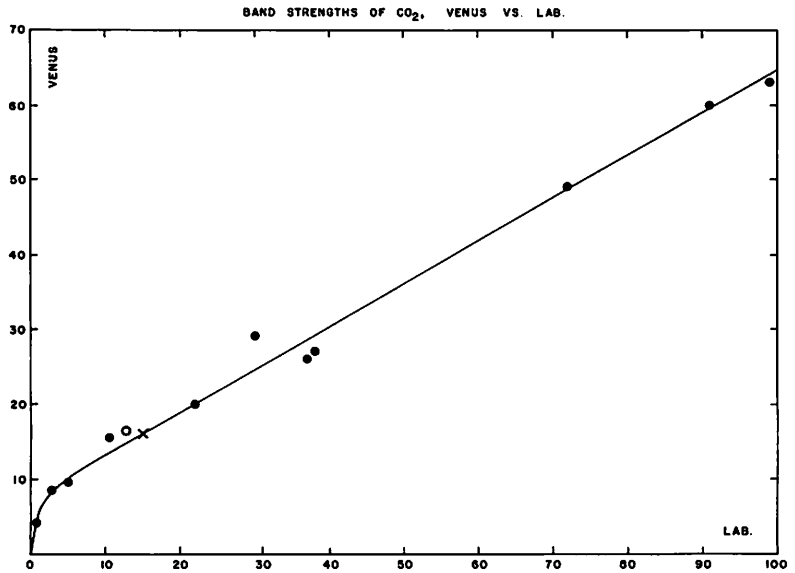

Fig. 22. Relation between CO_2 band strength in the Venus spectrum (June 17, 1962) and a laboratory spectrum similar to that reproduced in Figure 17. Data taken from Table 2. Each band is represented by a dot. The isotopic band $3\nu_3$ of $^{13}CO_2$ is shown as a cross; the $2\nu_3$ band of $^{12}C^{18}O^{16}O$ is shown as an open circle.

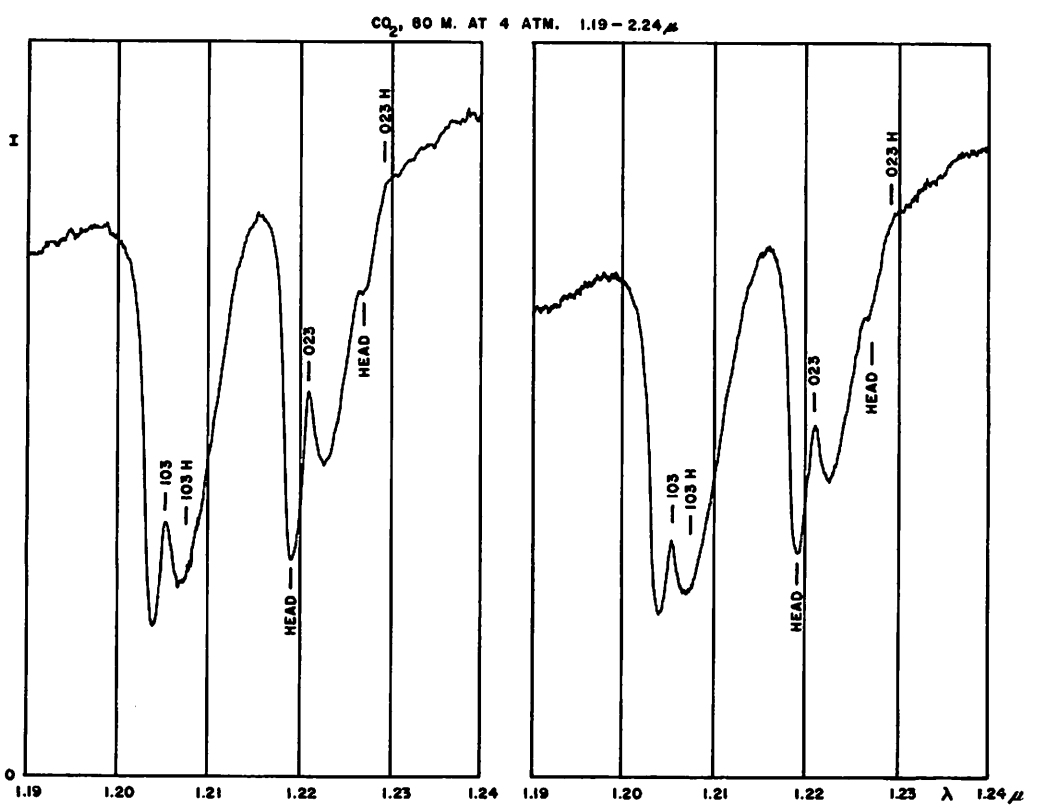

Fig. 23. Laboratory spectra of the 103 and 023 bands of CO_2 showing the hot band 023H at 295°K. Dispersion and resolution match the Venus spectra of Figures 8 and 9.

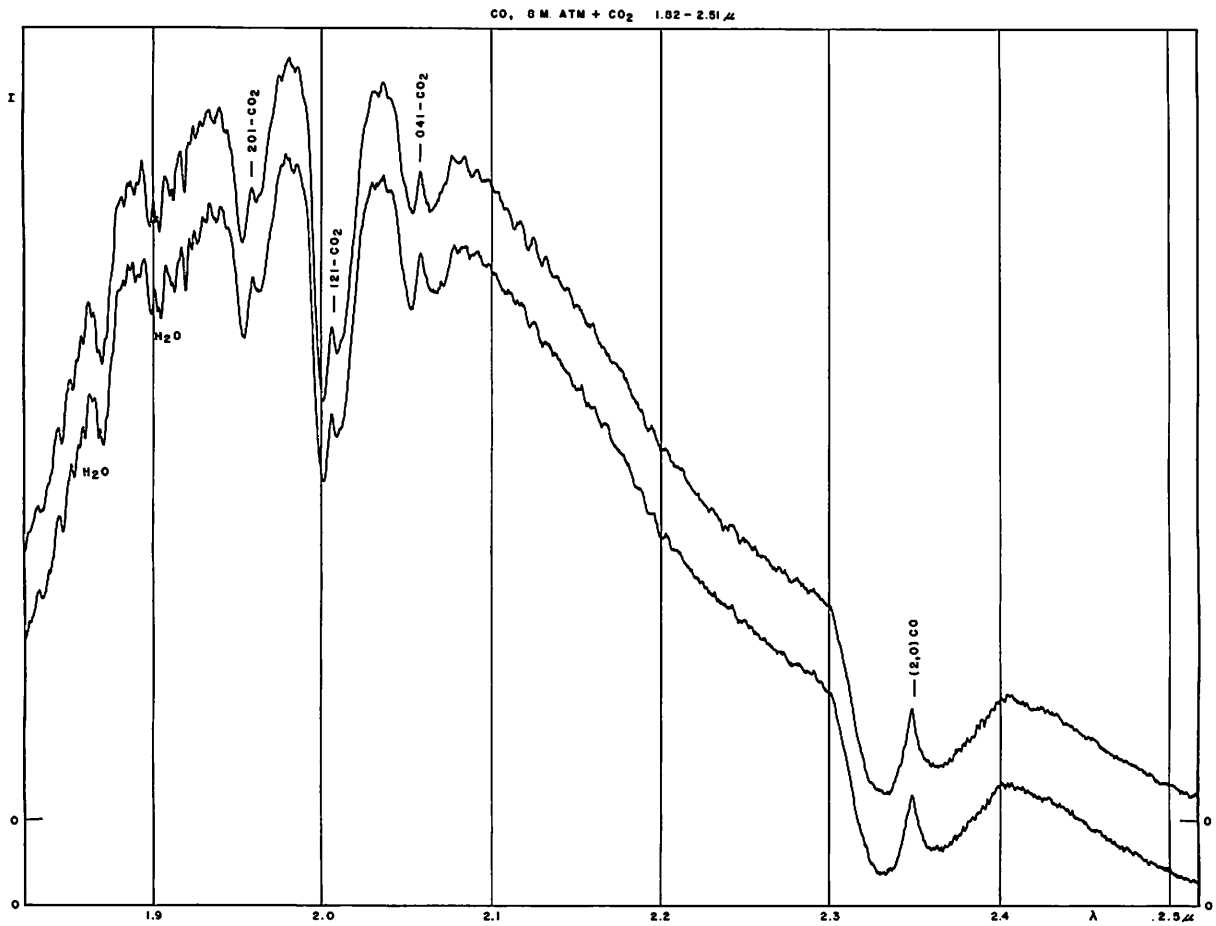

Fig. 24. Two consecutive runs of CO, pathlength 8 meters, pressure 1 atm., 1.82-2.51μ. Grating 2μ, filter $\lambda > 1.8\mu$, cell 0.25 mm, slit 0.3 mm, $\tau = 3$ seconds. The CO is contaminated with CO_2 and water vapor.

The determination of the isotope ratio from direct comparisons between the two $3\nu_3$ bands is difficult since the equivalent pathlength in the Venus atmosphere depends on the band strength itself. This is not true for laboratory spectra since the pathlength traversed is necessarily the same for both weak and strong bands. However, if the isotopic band fits the relationship of Figure 22, it means that the isotope ratio is the same on Venus as on the Earth. If not, the equivalent laboratory intensity of the isotopic Venus band may be found and the abundance ratio determined from laboratory tests with different pathlengths.

It is seen that the $3\nu_3$ isotopic band falls closely to the curve of Figure 22. The estimated precision of the Venus measure is $\pm$ 10 per cent, corresponding to $\pm$ 20 per cent in equivalent width in the laboratory intensity, as found from the local slope of the curve. Within this precision, the isotope ratio of $^{13}C/^{12}C$ is the same on Venus and on the Earth. Better precision should be obtainable in a very dry winter atmosphere.

(c) The oxygen isotope ratio $^{18}O/^{16}O$ can, at present, be determined from one band only, $2\nu_3$, the other bands being too badly blended (cf. Table 1 and the spectral records reproduced). The method used is the same as for the carbon isotope ratio, i.e., differentially, Earth vs. Venus. The equivalent width of the band has been measured on Venus spectrum Figure 4 and the laboratory spectra shown in Figure 19. The resulting data have been entered in Table 2 and Figure 22. It is seen that the isotope ratio is equal to that on the Earth within the error of measurement.

(d) The hot bands arising from the ν_2 level $\Pi_u(01^10)$ are quite prominent in the Venus spectrum wherever they are relatively free from blending. The best case is 023H, observed in the laboratory by Herzberg and Herzberg (1953, p. 1038), and well shown in the Venus spectrum on our Figures 1, 8,

and 9. It is better separated from the corresponding cold band than its twin member of the diade, 103, also well shown in the spectral plate reproduced by Herzberg and Herzberg. A separate laboratory study will be made to calibrate the Venus 023H band in terms of temperature. It is seen by comparison with Figures 17, 18 and 23 that the Venus temperature is considerably higher than the laboratory temperature of about 300°K.

(e) Of interest also is the determination of the maximum CO content in the Venus atmosphere, consistent with the spectra here reproduced. The necessary laboratory comparisons are given in Figures 24 and 25. From the observed strength of the $\lambda = 2.35\mu$ band of CO, the upper limit of 10 cm atm. NPT is found, implying an approximate upper limit of one-fourth of this amount for a vertical column in the Venus atmosphere. The (3,0) band of CO was also observed in the laboratory, but it is an order of magnitude weaker than the (2,0) band and has, moreover, the same wavelength as the (22°1) band of CO_2 at 1.575μ. It is therefore unsuitable for the determination of the CO content of Venus. The upper limit of about 3 cm for the Venus atmosphere represents an advance of about 30 x in the threshold limit compared to the author's 1948 result.

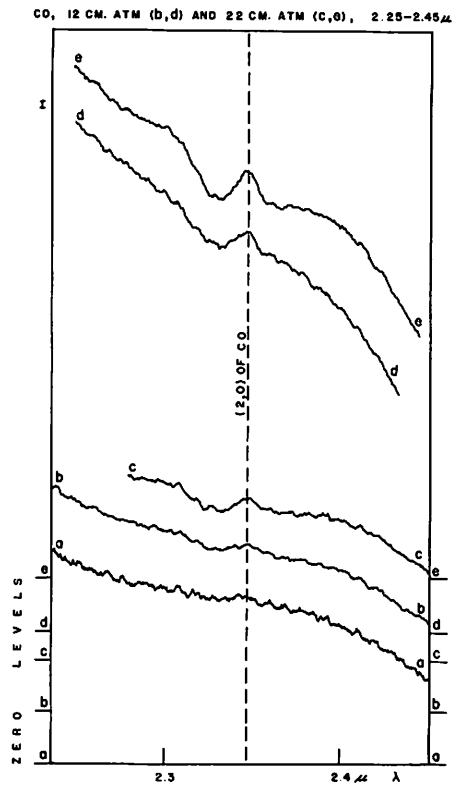

Fig. 25. Laboratory spectra of CO at 1 atm., 2.25-2.45μ, 2μ grating, filter $\lambda > 1.8\mu$, 0.3 mm slit, 0.25 mm cell. Same scale as Figure 24. (*a*) blank run; (b) 12 cm, g = 6-1, τ = 6 sec.; (c) 22 cm, g = 6-1, τ = 6 sec.; (d) 12 cm, g = 6-3, τ = 12 sec.; (e) 22 cm, g = 6-3, τ = 12 sec. (g is gain setting.)

5. *Comparison of Interferometer and Spectrometer*

Because of the current interest in the use of a Michelson interferometer in IR spectral scanning and the claims made for its "great advantage over conventional spectrometers," a brief discussion of the relative efficiency of the two methods is given here. Gebbie *et al.* used a time constant of ½ second, not very different from that used by the writer, and a rotating sector to modulate the received radiation, also as used in the spectrometer.

Let n be the number of spectral elements scanned (n may be 100-5000). The noise of the PbS cell is independent of the signal, except for very bright sources. For a selected time constant (say, $\simeq 1$ second) the uncertainty of the measure will therefore be the same for the total energy

$$\sum_1^n e_i = E \pm \sigma \qquad (1)$$

as for the interferometer reading at any time t:

$$\sum_1^n a_i e_i = E_t \pm \sigma. \qquad (2)$$

The coefficients a_i are known trigonometric functions of the time, essentially $\sin^2$ curves, with $0 \leq a_i \leq 1$. If the interferometer operates during n elementary intervals j (each equal to the time constant), as does the spectrometer, we shall in fact have n linear equations with n unknowns, all of the form (2). For the one-channel spectrometer

$$a_{ij} = 0 \ (i \neq j); \text{ and } a_{jj} = 1, \text{ with } j = 1, \ldots, n, \qquad (3)$$

which, because of the larger coefficients of the unknowns, will give a greater precision for the unknowns e_i than equation (2). Numerical experiments indicate that in the use of the interferometer the precision of equation (3) will be approached within a factor between 1 and 2. Thus, while no significant loss is incurred compared to the one-channel spectrometer, the interferometer is definitely not more efficient.

One may inquire, however, whether the interferometer might not disclose sharp absorption features more easily than the spectrometer even if it be granted that the energies themselves (i.e., the ordinates in a spectral plot) are not precisely determined.

In other words, while the shape of the continuum might be uncertain, sharp local gradients could possibly be emphasized. To some extent this appears to be the case. The first part of the interferogram determines the gross features, therefore the shape of the continuum; but because it is based on few observations, each possessing the standard error σ, the continuum is not well defined. No accurate spectrophotometry on the derived spectra will therefore be possible. However, sharp local gradients will be emphasized and will appear in the computed spectrum. While it is true that the detector is linear and able to record simultaneously a large number of frequencies without an increase in total noise, the resolution of each of these frequencies from the sum with the precision in the intensity of $\pm\sigma$ will require a length of interferogram that is proportional to n. The assumption that each element of the interferogram contains this information for all n frequencies cannot be valid since the total information content of each element must be constant and not dependent on n, which is arbitrary. Therefore, apart from numerical factors of the order of unity, the two methods of scanning are found to be equivalent in efficiency.

For a photoelectric detector the case for the interferometer is worse. Since the mean value of a_i is ½, the statistical fluctuations in equation (2) will on the average be $\pm\sigma_1\sqrt{n/2}$, not $\pm\sigma_1$, if σ_1 is the average uncertainty of one spectral element measured singly. Hence the factor in favor of the one-channel spectrometer will be $\sqrt{n/2}$ times greater than in the photoconductive case.

In astronomical applications there is an additional loss for the interferometer, by an unknown amount, stemming from the fact that the source itself is not strictly constant. For instance, astronomers familiar with IR observations have noted the presence of cloud-sized airmasses of increased water-vapor content, moving through a sky that seems optically entirely clear. This seems to occur when certain layers in the upper atmosphere either have contained visible clouds that have recently evaporated or are close to forming new clouds. When such "vapor clouds" cross the line of sight they will momentarily deepen the telluric lines in an ordinary spectrometer record, but no further harm is done. In an interferogram, however, they will cause fluctuations that in the analysis are attributed to absorption features all through the spectrum. Sudden seeing fluctuations or imperfections in the guiding will have similar effects. The troubles are localized in a spectrogram and are immediately spotted by an attentive observer who then has the opportunity to make another record of the defective part; but they will remain unnoticed and will be erroneously interpreted in the interferogram. These effects may be responsible for the features shown in the spectra of Venus by Gebbie *et al.* (1962) between 1.6-1.8μ and 2.2-2.4μ. The effects may be reduced, but not eliminated, by the use of narrow-band filters which exclude the heaviest H_2O absorptions.

The interferometer has a major advantage over the spectrometer on extended sources, such as nebulae or the zodiacal light, since no slit is required. For such objects also the guiding is less critical. It may well be that here the advantages over the spectrometer far outweigh the disadvantages, at least when photoconductive detectors are used.

The efficiency of the one-channel spectrometer itself can be surpassed by the use of a multi-channel detector (cf. p. 19). This device increases the efficiency proportionally to the number of channels used.

Acknowledgments.—The writer is much indebted to the administration of the Kitt Peak National Observatory for the use of the 36-inch telescope for several brief observing runs, culminating in the June, 1962, run; and to the Director of the McDonald Observatory for the generous use of the 82-inch telescope during several recent sessions, particularly the August, 1962, run. Dr. G. Herzberg, Head of the Division of Physics, National Research Council of Canada, greatly assisted our program by the loan of the 2-meter multiple-path absorption tube (used in the work by Courtoy referred to). He also suggested to us the classification of the $\lambda = 2.15\mu$ band of CO_2 as did, independently, Dr. W. S. Benedict. Messrs. Binder and Cruikshank assisted in the Kitt Peak runs and in obtaining the laboratory spectra; and Mr. Binder assisted in the two-week McDonald run. Mrs. Fabe and Mrs. Scheer prepared the spectral records for reproduction. I am indebted to Dr. A. B. Meinel for data on the energy diagram of CO_2. Mr. T. Owen was responsible for the installation of the Herzberg absorption tube and for the development of the accessories; he also assisted in the laboratory runs. The earlier phases of this work were carried out under Air Force Contract No. AF 19(604)7260; the later phases were sponsored by the National Aeronautics and Space Administration (NsG 161-61).

REFERENCES

Caughlan, G. R., and Fowler, W. A. 1962, *Ap. J., 136,* 453.

Courtoy, C. P. 1957, *Canadian J. Phys., 35,* 608.

————. 1959, "Spectre Infrarouge a Grande Dispersion et Constantes Moleculaires du CO_2," *Ann. Soc. Sci. de Bruxelles, 73,* 5-203.

Fowler, W. A., Greenstein, J. L., and Hoyle, F. 1962, *Geophys. J., 6,* 148.

Gebbie, H. A., Delbouille, L., and Roland, G. 1962, *M.N., 123,* 497.

Gebbie, H. A., Roland, G., and Delbouille, L. 1961, *Nature, 191,* 264.

Herzberg, G., and Herzberg, L. 1953, *J. Opt. Soc. America, 43,* 1037-1044.

Kuiper, G. P. 1947, *Ap. J., 106,* 252, Figs. 3 and 4.

————. 1948, *The Atmospheres of the Earth and Planets,* ed. G. P. Kuiper (1st ed.; Chicago: University of Chicago Press), p. 331.

————. 1952, *ibid.,* 2d ed., pp. 370-371.

McKellar, A. 1960, *Stellar Atmospheres,* ed. J. L. Greenstein (Chicago: University of Chicago Press), p. 579.

Plyler, E. K., Tidwell, E. D., and Benedict, W. S. 1962, *J. Opt. Soc. America, 52,* 1017.

Sinton, W. M. 1961, *Planets and Satellites* (Chicago: University of Chicago Press), p. 433, Fig. 3, and References.